

Fluctuations of a one-dimensional polynuclear growth model in a half space

T. Sasamoto^{*} and T. Imamura[†]

*Department of Physics, Tokyo Institute of Technology,
Oh-okayama 2-12-1, Meguro-ku, Tokyo 152-8551, Japan*

*Department of Physics, Graduate School of Science,
University of Tokyo,
Hongo 7-3-1, Bunkyo-ku, Tokyo 113-0033, Japan*

Abstract

We consider the multi-point equal time height fluctuations of a one-dimensional polynuclear growth model in a half space. For special values of the nucleation rate at the origin, the multi-layer version of the model is reduced to a determinantal process, for which the asymptotics can be analyzed. In the scaling limit, the fluctuations near the origin are shown to be equivalent to those of the largest eigenvalue of the orthogonal/symplectic to unitary transition ensemble at soft edge in random matrix theory.

[Keywords: polynuclear growth; KPZ universality class; random matrices; Tracy-Widom distribution; Airy process]

^{*}e-mail: sasamoto@stat.phys.titech.ac.jp

[†]e-mail: imamura@monet.phys.s.u-tokyo.ac.jp

1 Introduction

The problems of random surface growth have been an important subject of non-equilibrium statistical physics [1,2]. Interestingly, surfaces show universal statistical behaviors, depending on which mechanism plays a major role in growth. Among them is the Kardar-Parisi-Zhang (KPZ) universality class [3]. Though in many cases it is not enough to describe the growth of real materials, the KPZ universality class gives a satisfactory understanding of many growth models such as the Eden model, and hence plays a prominent role in theoretical study of growing surfaces.

It is difficult to study the KPZ universality class analytically for general dimension. In one spatial dimension, however, some exact results had been obtained. For instance, the exponents are already obtained in [3] based on dynamical renormalization group techniques. These have been further confirmed by exact solutions for the models in the KPZ universality class [4,5]. We will also restrict our attention to one spatial dimensional case in this article.

Recently, more refined information about the fluctuation properties of the 1+1 dimensional KPZ universality class have been obtained [6, 7, 8, 9, 10, 11, 12, 13, 14, 15]. For some important quantities such as the height fluctuation, not only the exponents but also the scaling functions are obtained. The whole new developments originate from the work [16] on the statistics of the longest increasing subsequence in a random permutation, which has turned out to be closely related to the random surface growth models [17].

The polynuclear growth (PNG) models are known to belong to the KPZ universality class [1, 2]. The PNG models are simple models which describe layer by layer random surface growth. In its standard version, a nucleation of a layer with height one occurs with rate two per unit length. After a nucleation, the layer grows laterally in both directions from the nucleation point with unit speed. In addition, there occur nucleations with rate two on already existing layers. A discrete version of the PNG model was introduced in [18] and studied further in [19]. The discrete PNG model has a close relationship with the asymmetric simple exclusion process (ASEP) [6, 13].

In [9,7,8], the height fluctuation of the PNG model at a given time and a given position was studied. It turned out that the fluctuation strongly depends on the geometry of the models. For instance, for the model in the infinite space, the fluctuation at the origin is described by the GUE Tracy-Widom distribution in random matrix theory [20,21]. On the other hand, for the model in a half space with an external source at the origin, it is described by the GOE/GSE Tracy-Widom distributions [22] or by the Gaussian. Models with other geometries are also considered in [7, 8]. These are based on the results in [9, 23, 24, 25], in which the longest increasing subsequence problem with some symmetries are considered.

For the models in the infinite space, multi-point equal time height fluctuations are studied by introducing the multi-layer version of the PNG model in [14] for the continuous time case and in [19] for the discrete time case. It is shown that the scaling limit is described by the Airy process, which is closely related to the dynamics of the rightmost particle of the Dyson's Brownian motion model [26].

In this article we study the multi-point equal time height fluctuations of the PNG model in a half space with external source at the origin. As mentioned above, the fluctuation

at a single point has already been considered in [25, 7]. At the origin, it is given by the GOE/GSE Tracy-Widom distribution whereas at other points, it is the GUE Tracy-Widom distribution. But the multi-point fluctuation has not been studied. Following the ideas of [27, 14], we introduce the multi-layer PNG model. In the scaling limit we will show that the crossover between the fluctuation at the origin and that in the bulk corresponds to the orthogonal/symplectic to unitary transition at soft edge in random matrix theory [28].

The outline of the paper is as follows. In the next section, the model we consider is defined. In section 3, a determinantal process is considered. Section 4 deals with the scaling limit of the models. In section 5, the results for the model without external source at the origin are summarized. The standard PNG model in a half space can be considered by taking the limit for the discrete model. This is done in section 6. Some discussions, conjectures and Monte-Carlo results are given in section 7, followed by the conclusion in the last section.

2 Model

Let $r \in \mathbb{N} = \{0, 1, 2, \dots\}$ and $t \in \mathbb{N}$ denote the discrete space and time coordinates respectively and $h(r, t)$ the height of the surface at position r and at time t . Our model lives in a half space $r \in \mathbb{N}$, but we can extend $h(r, t)$ to the whole space by setting $h(r, t) = h(-r, t)$ for $r \in \mathbb{Z}$, i.e. the height is symmetric under the reflection with respect to the origin. We can further extend $h(r, t)$ to all $r \in \mathbb{R}$ by setting $h(r, t) = h([r], t)$. Then the height looks symmetric under the reflection with respect to $r = 1/2$, i.e. $h(r, t) = h(1-r, t)$ for $r \in \mathbb{R} \setminus \mathbb{Z}$. The model considered in this article is described as follows. Initially at time $t = 0$ we have a flat substrate. At an odd time $t = 1, 3, \dots$, nucleations occur at even sites $r = 0, \pm 2, \dots, \pm t - 1$. At the origin, a nucleation of a height k ($\in \mathbb{N}$) happens with the probability $(1 - \gamma\sqrt{q})(\gamma\sqrt{q})^k$ where $0 < q < 1$ and $0 \leq \gamma < 1/\sqrt{q}$. For the height to be symmetric, nucleations at other points should be symmetric with respect to the origin; if the nucleation of a height k occurs at r , so does at $-r$ as well. Each independent nucleation with height k occurs with probability $(1 - q)q^k$. At an even time $t = 2, 4, \dots$, nucleations occur at odd sites $r = \pm 1, \pm 3, \dots, \pm t - 1$. The nucleations are again synchronous with respect to the origin and a height of each independent nucleation is a geometric random variable with parameter q . In the meantime the steps grow laterally in both directions with unit speed. Sometimes a downstep and an upstep collide with each other, in which case the two steps merge to one with the higher height. See Fig. 1. As is clear, the parameter q is related to the frequency of nucleations in the bulk whereas the parameter γ represents the strength of the external source at the origin. The bigger γ is, the stronger the source is. In particular $\gamma = 0$ corresponds to the model without the external source at the origin.

Mathematically, our discrete PNG model can be defined by

$$h(r, t + 1) = \max(h(r - 1, t), h(r, t), h(r + 1, t)) + \omega(r, t + 1), \quad (2.1)$$

with the initial condition $h(r, 0) = 0, r \in \mathbb{Z}$. Here ω is the random variable which takes a

value in \mathbb{N} . $\omega(r, t) = 0$ if $t - r$ is even or if $|r| > t$, and

$$w(i, j) = \omega(i - j, i + j - 1), \quad (2.2)$$

$(i, j) \in \mathbb{Z}_+^2$ are geometric random variables. In our model, all $w(i, j)$'s are not independent as in [19], but a symmetry condition $w(i, j) = w(j, i)$ is imposed. The parameters of the independent geometric random variables are given by q (resp. $\gamma\sqrt{q}$) for off-diagonal (resp. diagonal) points,

$$\mathbb{P}[w(i, j) = k] = (1 - q)q^k, \quad 1 \leq j < i, \quad (2.3)$$

$$\mathbb{P}[w(i, i) = k] = (1 - \gamma\sqrt{q})(\gamma\sqrt{q})^k, \quad 1 \leq i, \quad (2.4)$$

for $k \in \mathbb{N}$. Introduction of $w(i, j)$ above is almost unnecessary for the following discussions, but useful to see the connection to the problems of last passage percolation and ASEP [9, 6, 25].

In the following, we devote our most discussions to the two special choices of γ where the detailed analysis of the model is possible. One choice is $\gamma = 1$, which is known to correspond to a critical point of the model [25]. The other is $\gamma = 0$, which corresponds to the model without the external source at the origin. In the following, the $\gamma = 1$ (resp. $\gamma = 0$) case will sometimes be referred to as the orthogonal (resp. symplectic) case because it will turn out to be related to the orthogonal (resp. symplectic) to unitary transition of symmetries in random matrix theory. The analysis of the two cases are quite analogous, so that we mainly consider the $\gamma = 1$ case in the sequel and summarize the results for the $\gamma = 0$ case in section 5.

We would like to know the statistical properties of $h(r, t)$. As already mentioned in the introduction, the fluctuation of the height at a single point is already known. It is given by the GOE Tracy-Widom distribution at the origin [25] and by the GUE Tracy-Widom distribution at other points [7]. In this article, we are interested in the crossover between these two. Following [18, 14, 19], we introduce the multi-layer version of the model which is defined as follows. In the original single-layer discrete PNG model, when two steps meet, the higher step takes over the lower one. The information of the lower step is lost. To keep this information, let us suppose that there was a second layer below the original layer from the outset. The height of the second layer remains -1 until a collision of steps happens at the first layer, at which time the nucleation for the second layer occurs just below the collision. The height of the nucleation is taken to be the height of the overlapped region of the higher and the lower steps which collide at the first layer. See Fig. 1. The steps in the second layer grows laterally in both directions with unit speed as in the first layer. The nucleations at the second layer are only due to collisions of steps at the first layer; there is no additional probabilistic nucleations. We denote the height of the second layer at position r and at time t as $h_1(r, t)$. One can further suppose that there were infinitely many layers below the first layer, equally spaced at time 0 and successively construct $h_i(r, t)$ for $i = 2, 3, \dots$. We also set $h(r, t) = h_0(r, t)$. This is the multi-layer PNG model. An example of the whole height configurations is given in Fig. 2.

In the following, we mainly consider an even time, which is fixed to $t = M = 2N$ until the asymptotics is considered. There are infinitely many lines, but for time $t = M$ the number of lines which are not straight is at most N . Moreover, there is a restriction, $h_i(M, M) = -i$ ($i = 0, 1, \dots, N - 1$). For each jump with length k of all layers, we associate a weight $(\sqrt{q})^k$. Since the whole configuration of the layers keep all information of nucleations, the product of all weights of all jumps in the multi-layer PNG at $t = M$ is given by

$$\prod_{i+j \leq 2N+1, i > j} q^{w(i,j)} \prod_{i=1}^N (\sqrt{q})^{w(i,i)}. \quad (2.5)$$

From now on, we change the way of looking at multi-layer heights. The space coordinate r in the original setting will be interpreted as the time coordinate. The height coordinate will be interpreted as the space coordinate and is represented as x . We set $h_i(r, t) = x_{i+1}^r$ for $i = 0, 1, \dots, N - 1$ and $r = 0, 1, \dots, M$, and regard the height lines as paths of particles. Let us denote the collection of the positions of particles at time r as $x^r = (x_1^r, \dots, x_N^r)$ where $x_1^r > \dots > x_N^r$, and a collection of them for all times as $\bar{x} = (x^0, \dots, x^M)$.

In what follows we use $\alpha = \sqrt{q}$. Suppose that, when the the particle picture of heights are employed, the x and r axes are pointing the right and the up respectively. Then at odd times, particles move to the right. The transition weight of a particle from x at time $2u$ to y at time $2u + 1$ is given by

$$\phi_{2u, 2u+1}(x, y) = \begin{cases} (1 - \alpha)\alpha^{y-x}, & y \geq x, \\ 0, & y < x. \end{cases} \quad (2.6)$$

At even times, they move to the left. The transition weight for each particle is

$$\phi_{2u-1, 2u}(x, y) = \begin{cases} 0, & y > x, \\ (1 - \alpha)\alpha^{x-y}, & y \leq x. \end{cases} \quad (2.7)$$

Then, according to the Karlin-McGregor theorem [29, 30], the weight of non-intersecting paths of n particles which ends at $x_i^M = 1 - i$ is given by

$$w_{n,M}(\bar{x}) = \prod_{r=0}^{M-1} \det(\phi_{r,r+1}(x_i^r, x_j^{r+1}))_{i,j=1}^n, \quad (2.8)$$

with the restriction $x_i^M = 1 - i$. The weight is written in a determinantal form, and hence the corresponding process is called a determinantal process. Notice that the weight in (2.8) with $n = N$ is slightly different from the weight of the multi-layer PNG model because some configurations contained in (2.8) are not allowed in the multi-layer PNG model where there are infinitely many particles. On the other hand, if we take the limit $n \rightarrow \infty$ from the beginning, there would appear another difficulty due to the infinity of the number of particles. Thus, for simplicity of the treatment, we approximate the weight of the multi-layer PNG model by (2.8) for the moment and take the limit $n \rightarrow \infty$ afterwards when it

becomes easy. The simple determinantal expression in (2.8) allows us to perform a detailed analysis of the model. If we took diagonal parameters to be more general as in (2.4), the expression would become more complicated.

For later use, we introduce the generating function of $\phi_{r,r+1}$,

$$f_{2u}(z) = \sum_{k \in \mathbb{Z}} \phi_{2u,2u+1}(k) z^k = \frac{1 - \alpha}{1 - \alpha z}, \quad (2.9)$$

$$f_{2u-1}(z) = \sum_{k \in \mathbb{Z}} \phi_{2u-1,2u}(k) z^k = \frac{1 - \alpha}{1 - \alpha/z}. \quad (2.10)$$

Let us denote the Fourier coefficient of a function $a(z)$ as $\hat{a}(k)$ like

$$a(z) = \sum_{k \in \mathbb{Z}} \hat{a}(k) z^k. \quad (2.11)$$

For instance one sees

$$\phi_{2u,2u+1}(x, y) = \hat{f}_{2u}(y - x), \quad (2.12)$$

$$\phi_{2u-1,2u}(x, y) = \hat{f}_{2u-1}(y - x). \quad (2.13)$$

In addition, for a product,

$$f_{r_1, r_2}(z) = \prod_{l=r_1}^{r_2} f_l(z), \quad (2.14)$$

the Fourier coefficient,

$$\phi_{r_1, r_2}(x, y) = \hat{f}_{r_1, r_2}(y - x), \quad (2.15)$$

represents the transition weight of a particle between (r_1, x) and (r_2, y) . Notice that when $r_1 = r_2 = r$ one has

$$\phi_{r,r}(x, y) = \delta_{xy}. \quad (2.16)$$

Before going to the next section, a remark is in order. Although we have employed the situation where the geometric random variables are given by a single parameter q , up to some point, it is easy to generalize our discussions to the case where

$$\mathbb{P}[w(i, j) = k] = (1 - a_i a_j)(a_i a_j)^k, \quad 1 \leq j < i, \quad (2.17)$$

$$\mathbb{P}[w(i, i) = k] = (1 - a_i) a_i^k, \quad 1 \leq i, \quad (2.18)$$

with $0 < a_i < 1$ for all i . Then (2.9),(2.10) are replaced by

$$f_{2u}(z) = \frac{1 - a_{N+u+1}}{1 - a_{N+u+1} z}, \quad (2.19)$$

$$f_{2u-1}(z) = \frac{1 - a_{N-u+1}}{1 - a_{N-u+1}/z}, \quad (2.20)$$

with the transition weight of a particle again given by (2.12),(2.13). It should be noted that our free parameters are only a_j 's; for the case in [18], there are two sets of free parameters a_j, b_j .

3 Determinantal Process and Kernel

Let us consider the weight of non-intersecting paths given by

$$w_{n,M}(\bar{x}) = \prod_{r=0}^{M-1} \det(\phi_{r,r+1}(x_i^r, x_j^{r+1}))_{i,j=1}^n, \quad (3.1)$$

where x_i^M ($i = 1, 2, \dots, n$) is fixed. As for x_i^0 , there is no restriction. This is the main difference between our model and the model in [19] in which x_i^0 is also fixed. The matrix element $\phi_{r,r+1}(x_i^r, x_j^{r+1})$ is the transition weight of a particle between (r, x_i^r) and $(r+1, x_j^{r+1})$. Our main focus is on the special case in (2.6),(2.7), but the results of this section do not depend on a specific choice of ϕ . For instance, when particles can hop only to nearest neighbor sites for each time, the determinantal process is nothing but the vicious walks studied in [31, 32, 33]. Hence our discussions below can immediately be applied to the problems as well.

The partition function is defined as

$$Z_{n,M} = \frac{1}{(n!)^M} \sum_{\bar{x}} w_{n,M}(\bar{x}). \quad (3.2)$$

The probability of the non-intersecting paths reads

$$p_{n,M}(\bar{x}) = \frac{1}{(n!)^M Z_{n,M}} w_{n,M}(\bar{x}). \quad (3.3)$$

Let $g(r, x)$ ($r = 1, \dots, M$) be some function. In this section, we show

Proposition 3.1.

$$\sum_{\bar{x}} \prod_{r=0}^{M-1} \prod_{j=1}^n (1 + g(r, x_j^r)) p_{n,M}(\bar{x}) = \sqrt{\det(1 + K_1 g)}, \quad (3.4)$$

where the determinant on the right hand side is the Fredholm determinant,

$$\det(1 + K_1 g) = \sum_{k=0}^{\infty} \frac{1}{k!} \sum_{r_1=1}^M \sum_{x_1} \sum_{j_1=1,2} \cdots \sum_{r_k=1}^M \sum_{x_k} \sum_{j_k=1,2} g(r_1, x_1) \cdots g(r_k, x_k) \det(K_1(r_l, x_l; r_{l'}, x_{l'}))_{l,l'=1}^k, \quad (3.5)$$

and K_1 is the 2×2 matrix kernel,

$$K_1(r_1, x_1; r_2, x_2) = \begin{bmatrix} S_1(r_1, x_1; r_2, x_2) & D_1(r_1, x_1; r_2, x_2) \\ I_1(r_1, x_1; r_2, x_2) & S_1(r_2, x_2; r_1, x_1) \end{bmatrix}, \quad (3.6)$$

with the matrix elements being

$$S_1(r_1, x_1; r_2, x_2) = \tilde{S}_1(r_1, x_1; r_2, x_2) - \phi_{r_1, r_2}(x_1, x_2), \quad (3.7)$$

$$\tilde{S}_1(r_1, x_1; r_2, x_2) = - \sum_{i,j=1}^n \phi_{r_1, M}(x_1, x_i^M) (A_1^{-1})_{i,j} G_1(r_2, x_2; M, x_j^M), \quad (3.8)$$

$$I_1(r_1, x_1; r_2, x_2) = \tilde{I}_1(r_1, x_1; r_2, x_2) - G_1(r_1, x_1; r_2, x_2), \quad (3.9)$$

$$\tilde{I}_1(r_1, x_1; r_2, x_2) = - \sum_{i,j=1}^n G_1(r_1, x_1; M, x_i^M) (A_1^{-1})_{i,j} G_1(r_2, x_2; M, x_j^M), \quad (3.10)$$

$$D_1(r_1, x_1; r_2, x_2) = \sum_{i,j=1}^n \phi_{r_1, M}(x_1, x_i^M) (A_1^{-1})_{i,j} \phi_{r_2, M}(x_2, x_j^M). \quad (3.11)$$

Here

$$(A_1)_{ij} = \sum_{y_1, y_2} \text{sgn}(y_2 - y_1) \phi_{0, M}(y_1, x_i^M) \phi_{0, M}(y_2, x_j^M), \quad (3.12)$$

$$G_1(r_1, x_1; r_2, x_2) = \sum_{y_1, y_2} \text{sgn}(y_2 - y_1) \phi_{0, r_1}(y_1, x_1) \phi_{0, r_2}(y_2, x_2). \quad (3.13)$$

The expression for general $K_1(r_i, x_i; r_j, x_j)$ ($i, j = 1, 2, \dots, M$) has the same form as $K_1(r_1, x_1; r_2, x_2)$.

Remark. The subscript 1 refers to the fact that this case is related to the orthogonal-unitary transition in random matrix theory. If we take $g(r, x) = -\chi_{J_r}(x)$ ($r = 1, 2, \dots, M$), where χ_{J_r} is the characteristic function of J_r , (3.4) gives the probability that there is no particle on $J_1 \times \dots \times J_M$. It should also be remarked that at this stage the infinite particles limit is taken easily. One only replaces the summation, $\sum_{i,j=1}^n$, in (3.8),(3.10),(3.11) with $\sum_{i,j=1}^{\infty}$.

Proof. We derive (3.4) by generalizing the methods of [19] and [34]. Let us define

$$Z_{n, M}[g] = \frac{1}{(n!)^M} \sum_{\bar{x}} \prod_{r=0}^{M-1} \prod_{j=1}^n (1 + g(r, x_j^r)) w_{n, M}(\bar{x}). \quad (3.14)$$

Remark $Z_{n, M}[0] = Z_{n, M}$ so that

$$\sum_{\bar{x}} \prod_{r=0}^{M-1} \prod_{j=1}^n (1 + g(r, x_j^r)) p_{n, M}(\bar{x}) = \frac{Z_{n, M}[g]}{Z_{n, M}[0]}. \quad (3.15)$$

By repeated use of the Heine identity,

$$\frac{1}{n!} \sum_x \det(\phi_i(x_j))_{i,j=1}^n \det(\varphi_i(x_j))_{i,j=1}^n = \det \left(\sum_X \phi_i(X) \varphi_j(X) \right)_{i,j=1}^n, \quad (3.16)$$

one has

$$Z_{n,M}[g] = \sum_{x_1^0 > \dots > x_n^0} \det \left(\sum_{X_1, \dots, X_{M-1}} (1 + g(0, x_i^0)) \phi_{0,1}(x_i^0, X_1) (1 + g(1, X_1)) \cdots \right. \\ \left. \phi_{M-2, M-1}(X_{M-2}, X_{M-1}) (1 + g(M-1, X_{M-1})) \phi_{M-1, M}(X_{M-1}, x_j^M) \right)_{i,j=1}^n. \quad (3.17)$$

Now, using another identity [35, 34],

$$\left(\sum_{x_1 > \dots > x_n} \det(\phi_i(x_j))_{i,j=1}^n \right)^2 = \det \left(\sum_{y_1, y_2} \operatorname{sgn}(y_2 - y_1) \phi_i(y_1) \phi_j(y_2) \right)_{i,j=1}^n, \quad (3.18)$$

one finds

$$Z_{n,M}[g]^2 = \det \left(\sum_{y_1, y_2} \operatorname{sgn}(y_2 - y_1) \sum_{X_1, \dots, X_{M-1}} (1 + g(0, y_1)) \phi_{0,1}(y_1, X_1) \cdots \phi_{M-1, M}(X_{M-1}, x_i^M) \right. \\ \left. \sum_{\tilde{X}_1, \dots, \tilde{X}_{M-1}} (1 + g(0, y_2)) \phi_{0,1}(y_2, \tilde{X}_1) \cdots \phi_{M-1, M}(\tilde{X}_{M-1}, x_j^M) \right)_{i,j=1}^n \\ = \det \left(\sum_{y_1, y_2} \operatorname{sgn}(y_2 - y_1) \sum_{X_0, \dots, X_{M-1}} \phi_{0,0}(y_1, X_0) (1 + g(0, X_0)) \phi_{0,1}(X_0, X_1) \cdots \phi_{M-1, M}(X_{M-1}, x_i^M) \right. \\ \left. \sum_{\tilde{X}_0, \dots, \tilde{X}_{M-1}} \phi_{0,0}(y_2, \tilde{X}_0) (1 + g(0, \tilde{X}_0)) \phi_{0,1}(\tilde{X}_0, \tilde{X}_1) \cdots \phi_{M-1, M}(\tilde{X}_{M-1}, x_j^M) \right)_{i,j=1}^n. \quad (3.19)$$

For the second equality we used $\phi_{0,0}(x, y) = \delta_{x,y}$. We divide the (i, j) element of the matrix in the above determinant into four parts with or without factors of the form $g(r, X_r)$ or $g(\tilde{r}, \tilde{X}_r)$. We have

$$Z_{n,M}[g]^2 = \det \left((A_1)_{i,j} + (A_1^{(1)})_{i,j} + (A_1^{(2)})_{i,j} + (A_1^{(3)})_{i,j} \right)_{i,j=1}^n, \quad (3.20)$$

where $(A_1)_{i,j}$ is already defined in (3.12) and

$$(A_1^{(1)})_{i,j} = \sum_{y_1, y_2} \operatorname{sgn}(y_2 - y_1) \sum_{l=1}^M \sum_{0 \leq r_1 < \dots < r_l < M} \sum_{X_1, \dots, X_l} \phi_{0, r_1}(y_1, X_1) \\ \prod_{s=1}^{l-1} g(r_s, X_s) \phi_{r_s, r_{s+1}}(X_s, X_{s+1}) \cdot g(r_l, X_l) \phi_{r_l, M}(X_l, x_i^M) \cdot \phi_{0, M}(y_2, x_j^M), \quad (3.21)$$

$$\begin{aligned}
(A_1^{(2)})_{i,j} &= \sum_{y_1, y_2} \operatorname{sgn}(y_2 - y_1) \phi_{0,M}(y_1, x_i^M) \sum_{l=1}^M \sum_{0 \leq \tilde{r}_1 < \dots < \tilde{r}_l < M} \sum_{\tilde{X}_1, \dots, \tilde{X}_l} \phi_{0, \tilde{r}_1}(y_2, \tilde{X}_1) \\
&\quad \prod_{s=1}^{l-1} g(\tilde{r}_s, \tilde{X}_s) \phi_{\tilde{r}_s, \tilde{r}_{s+1}}(\tilde{X}_s, \tilde{X}_{s+1}) \cdot g(\tilde{r}_l, \tilde{X}_l) \phi_{\tilde{r}_l, M}(\tilde{X}_l, x_j^M), \tag{3.22}
\end{aligned}$$

$$\begin{aligned}
(A_1^{(3)})_{i,j} &= \sum_{y_1, y_2} \operatorname{sgn}(y_2 - y_1) \sum_{l=1}^M \sum_{0 \leq r_1 < \dots < r_l < M} \sum_{X_1, \dots, X_l} \phi_{0, r_1}(y_1, X_1) \\
&\quad \prod_{s=1}^{l-1} g(r_s, X_s) \phi_{r_s, r_{s+1}}(X_s, X_{s+1}) \cdot g(r_l, X_l) \phi_{r_l, M}(X_l, x_i^M) \\
&\quad \sum_{m=1}^M \sum_{0 \leq \tilde{r}_1 < \dots < \tilde{r}_m < M} \sum_{\tilde{X}_1, \dots, \tilde{X}_m} \phi_{0, \tilde{r}_1}(y_2, \tilde{X}_1) \\
&\quad \prod_{s=1}^{m-1} g(\tilde{r}_s, \tilde{X}_s) \phi_{\tilde{r}_s, \tilde{r}_{s+1}}(\tilde{X}_s, \tilde{X}_{s+1}) \cdot g(\tilde{r}_m, \tilde{X}_m) \phi_{\tilde{r}_m, M}(\tilde{X}_m, x_j^M). \tag{3.23}
\end{aligned}$$

Let us define

$$\varphi(r_1, x_1; r_2, x_2) = g(r_1, x_1) \phi_{r_1, r_2}(x_1, x_2), \tag{3.24}$$

$$\tilde{\varphi}(r_1, x_1; r_2, x_2) = \phi_{r_1, r_2}(x_1, x_2) g(r_2, x_2), \tag{3.25}$$

and

$$\phi_i(r, x) = \phi_{r, M}(x, x_i^M), \tag{3.26}$$

$$(G_1)_i(r, x) = G_1(r, x; M, x_i^M), \tag{3.27}$$

$$\begin{aligned}
\psi_i(r, x) &= \sum_{l=1}^M \sum_{r_2, \dots, r_l} \sum_{X_2, \dots, X_l} \phi_{r, r_2}(x, X_2) \prod_{s=2}^{l-1} \varphi(r_s, X_s; r_{s+1}, X_{s+1}) \cdot \varphi(r_l, X_l; M, x_i^M). \tag{3.28}
\end{aligned}$$

Then $(A_1^{(1)})_{i,j}$ can be rewritten as

$$\begin{aligned}
(A_1^{(1)})_{i,j} &= \sum_{l=1}^M \sum_{r_1=0}^{M-1} \dots \sum_{r_l=1}^{M-1} \sum_{X_1, \dots, X_l} G_1(r_1, X_1; M, x_j^M) g(r_1, X_1) \cdot \phi_{r_1, r_2}(X_1, X_2) \\
&\quad \prod_{s=2}^{l-1} \varphi(r_s, X_s; r_{s+1}, X_{s+1}) \cdot \varphi(r_l, X_l; M, x_i^M) \\
&= \sum_{r, x} g(r, x) \psi_i(r, x) G_1(r, x; M, x_j^M) \\
&= \sum_{r, x} g \psi_i \cdot (G_1)_j. \tag{3.29}
\end{aligned}$$

In the last expression, the dependence on r, x is omitted for notational simplicity. Noticing the antisymmetry of G_1 ,

$$G_1(r_1, x_1; r_2, x_2) = -G_1(r_2, x_2; r_1, x_1), \quad (3.30)$$

we can also rewrite $(A_1)_{i,j}^{(2)}$ and $(A_1)_{i,j}^{(3)}$ as

$$(A_1^{(2)})_{i,j} = - \sum_{r,x} g\psi_j \cdot (G_1)_i, \quad (3.31)$$

$$(A_1^{(3)})_{i,j} = - \sum_{r,x} g\psi_j \cdot G_1(g\psi_i), \quad (3.32)$$

where we used the notation,

$$(G_1 f)(r, x) = \sum_{r_1, x_1} G_1(r, x; r_1, x_1) f(r_1, x_1). \quad (3.33)$$

Hence we find

$$Z_{n,M}[g]^2 = \det \left((A_1)_{i,j} + \sum_{r,x} (g\psi_i \cdot (G_1)_j - g\psi_j \cdot (G_1)_i - g\psi_j \cdot G_1(g\psi_i)) \right)_{i,j=1}^n. \quad (3.34)$$

In view of (3.15), we divide this by

$$Z_{n,M}[0]^2 = \det A_1. \quad (3.35)$$

In the determinant this corresponds to multiplying by A_1^{-1} , say from the left. Let $\eta_i = \sum_j (A_1^{-1})_{i,j} \psi_j$, $\Psi_i = \sum_j (A_1^{-1})_{i,j} (G_1)_j$. Then

$$\left(\frac{Z_{n,M}[g]}{Z_{n,M}[0]} \right)^2 = \det \left(\delta_{i,j} + \sum_{r,x} (g\eta_i \cdot (G_1)_j - g\psi_j \cdot \Psi_i - g\psi_j \cdot G_1(g\eta_i)) \right)_{i,j=1}^n. \quad (3.36)$$

One notices that, if one introduces

$$B(i; r, x) = (-g\Psi_i - gG_1(g\eta_i), g\eta_i), \quad C(r, x; i) = \begin{pmatrix} \psi_i \\ (G_1)_i \end{pmatrix}, \quad (3.37)$$

this is equal to

$$\det \left(\delta_{i,j} + \sum_{r,x} B(i; r, x) C(r, x; j) \right)_{i,j=1}^n = \det(1 + BC). \quad (3.38)$$

Now we use a simple fact

$$\det(1 + BC) = \det(1 + CB). \quad (3.39)$$

The determinant on the left hand side is the determinant of a matrix of finite rank, whereas the one on the right hand side is the Fredholm determinant. We see

$$\det(1 + CB) = \det \begin{bmatrix} 1 - \sum_i \psi_i \otimes g\Psi_i - \sum_i \psi_i \otimes gG_1(g\eta_i) & \sum_i \psi_i \otimes g\eta_i \\ -\sum_i (G_1)_i \otimes g\Psi_i - \sum_i (G_1)_i \otimes gG_1(g\eta_i) & 1 + \sum_i (G_1)_i \otimes g\eta_i \end{bmatrix},$$

where we used the notation $a \otimes b$ for the operator with kernel of the form $a(r_1, x_1)b(r_2, x_2)$. The matrix in the determinant may be rewritten as a product of two matrices, leading to

$$\det \left(\begin{bmatrix} 1 - \sum_i \psi_i \otimes g\Psi_i & \sum_i \psi_i \otimes g\eta_i \\ -\sum_i (G_1)_i \otimes g\Psi_i - G_1g & 1 + \sum_i (G_1)_i \otimes g\eta_i \end{bmatrix} \begin{bmatrix} 1 & 0 \\ G_1g & 1 \end{bmatrix} \right). \quad (3.40)$$

The determinant of the right matrix is one, so that this equals

$$\det \left(1 + \begin{bmatrix} -\sum_i \psi_i \otimes g\Psi_i & \sum_i \psi_i \otimes g\eta_i \\ -\sum_i (G_1)_i \otimes g\Psi_i - G_1g & \sum_i (G_1)_i \otimes g\eta_i \end{bmatrix} \right). \quad (3.41)$$

Let us remember the definition of ψ_i in (3.28) and notice

$$\psi_i = \sum_{l=1}^M \tilde{\varphi}^{*(l-1)} * \phi_i = (1 - \tilde{\varphi})^{-1} * \phi_i, \quad (3.42)$$

$$g\psi_i = \sum_{l=1}^M \varphi^{*(l-1)} * (g\phi_i) = (1 - \varphi)^{-1} * (g\phi_i), \quad (3.43)$$

where

$$(f_1 * f_2)(r_1, x_1; r_2, x_2) = \sum_{r, x} f_1(r_1, x_1; r, x) f_2(r, x; r_2, x_2). \quad (3.44)$$

The determinant we are considering is now

$$\det \left(1 + \begin{bmatrix} (1 - \tilde{\varphi})^{-1} & 0 \\ 0 & 1 \end{bmatrix} \begin{bmatrix} -\sum_i \phi_i \otimes g\Psi_i & \sum_i \phi_i \otimes g(A_1^{-1}\phi)_i \\ -\sum_i (G_1)_i \otimes g\Psi_i - G_1g & \sum_i (G_1)_i \otimes g(A_1^{-1}\phi)_i \end{bmatrix} \begin{bmatrix} 1 & 0 \\ 0 & (1 - {}^t\varphi)^{-1} \end{bmatrix} \right). \quad (3.45)$$

Multiplying from the left by

$$1 = \det \begin{bmatrix} 1 - \tilde{\varphi} & 0 \\ 0 & 1 \end{bmatrix} \quad (3.46)$$

and from the right by

$$1 = \det \begin{bmatrix} 1 & 0 \\ 0 & 1 - {}^t\varphi \end{bmatrix}, \quad (3.47)$$

one gets

$$\begin{aligned}
& \left(\frac{Z_{n,M}[g]}{Z_{n,M}[0]} \right)^2 \\
&= \det \left(\begin{bmatrix} 1 - \tilde{\varphi} & 0 \\ 0 & 1 - {}^t\varphi \end{bmatrix} \right. \\
&\quad \left. + \begin{bmatrix} -\sum_{i,j} \phi_i \otimes (A_1^{-1})_{i,j}(G_1)_j & \sum_{i,j} \phi_i \otimes (A_1^{-1})_{i,j}\phi_j \\ -\sum_{i,j} (G_1)_i \otimes (A_1^{-1})_{i,j}(G_1)_j - G_1 & \sum_{i,j} (G_1)_i \otimes (A_1^{-1})_{i,j}\phi_j \end{bmatrix} g \right) \\
&= \det \left(1 + \begin{bmatrix} -\sum_{i,j} \phi_i \otimes (A_1^{-1})_{i,j}(G_1)_j - \phi & \sum_{i,j} \phi_i \otimes (A_1^{-1})_{i,j}\phi_j \\ -\sum_{i,j} (G_1)_i \otimes (A_1^{-1})_{i,j}(G_1)_j - G_1 & \sum_{i,j} (G_1)_i \otimes (A_1^{-1})_{i,j}\phi_j - {}^t\phi \end{bmatrix} g \right). \tag{3.48}
\end{aligned}$$

Recalling the definitions of ϕ_i and $(G_1)_i$ in (3.26) and (3.27), we see that (3.4) holds. \square

4 Scaling Limit

In this section we consider the scaling limit, where the universal properties of the model are expected to appear.

4.1 Generating Functions

To study the asymptotics of the kernel, we compute the generating functions of $\tilde{S}_1, \tilde{I}_1, D_1$.

First let us recall some basic facts about a Toeplitz matrix [36]. A Toeplitz matrix is a matrix A of the form,

$$A = \begin{bmatrix} a_0 & a_{-1} & a_{-2} & \cdots \\ a_1 & a_0 & a_{-1} & \\ a_2 & a_1 & a_0 & \cdots \\ \vdots & & \ddots & \ddots \end{bmatrix}. \tag{4.1}$$

It is useful to define a function,

$$a(z) = \sum_{k \in \mathbb{Z}} a_k z^k, \tag{4.2}$$

which is called the symbol of the Toeplitz matrix A . Conversely, for a given function $a(z)$, set $a_k = \hat{a}(k)$, the Fourier coefficient of the symbol $a(z)$. Then one can define the corresponding Toeplitz matrix (4.1), which will be denoted by $T(a)$. The inverse of A can be given in a compact fashion, if the symbol $a(z)$ has winding number zero and is Wiener-Hopf factorizable as

$$a(z) = a_+(z)a_-(z) \tag{4.3}$$

with

$$a_+(z) = \sum_{k=0}^{\infty} \hat{a}_+(k) z^k, \quad (4.4)$$

$$a_-(z) = \sum_{k=0}^{\infty} \hat{a}_-(k) z^{-k}. \quad (4.5)$$

In fact for a factorization (4.3) one has

$$A = T(a) = T(a_-)T(a_+). \quad (4.6)$$

In addition, the inverse of the matrix $T(a_{\pm})$ is simply given by

$$T(a_{\pm})^{-1} = T\left(\frac{1}{a_{\pm}}\right). \quad (4.7)$$

Hence the inverse of the matrix A is

$$A^{-1} = T\left(\frac{1}{a_+}\right)T\left(\frac{1}{a_-}\right). \quad (4.8)$$

To obtain the generating functions of $\tilde{S}_1, \tilde{I}_1, D_1$, we need the inverse of the matrix A_1 (3.12). As remarked below (3.13), for the multi-layer PNG model, the matrix A_1 should be taken to be an infinite dimensional one, which turns out to be a Toeplitz matrix. If we set

$$(A_1)_{ij} = \hat{a}(i - j), \quad (4.9)$$

the symbol is computed as

$$\begin{aligned} a_1(z) &= \sum_{k \in \mathbb{Z}} \hat{a}(k) z^k \\ &= \sum_{k, y_1, y_2} \hat{f}_{0,M}(1 - k - y_1) z^{-1+k+y_1} \cdot \text{sgn}(y_2 - y_1) z^{y_2 - y_1} \cdot \hat{f}_{0,M}(1 - y_2) z^{1-y_2} \\ &= f_{0,M}\left(\frac{1}{z}\right) s_1(z) f_{0,M}(z), \end{aligned} \quad (4.10)$$

where

$$s_1(z) = \sum_{k \in \mathbb{Z}} \text{sgn}(k) z^k = \frac{1+z}{1-z}. \quad (4.11)$$

In the second equality of (4.10), we use (2.15) and (3.12). The winding number of $a_1(z)$ is not zero and hence the formula (4.8) does not hold as it is in this case. But the difficulty can be overcome fairly easily. Let us first notice that $s_1(z)$ can be written in two ways as

$$s_1(z) = s_{1+}^{(1)}(z) s_{1-}^{(1)}(z) = s_{1+}^{(2)}(z) s_{1-}^{(2)}(z), \quad (4.12)$$

with

$$s_{1+}^{(1)}(z) = \frac{1+z}{1-z}, \quad s_{1-}^{(1)}(z) = 1, \quad (4.13)$$

$$s_{1+}^{(2)}(z) = 1, \quad s_{1-}^{(2)}(z) = -\frac{1+1/z}{1-1/z}. \quad (4.14)$$

Correspondingly, if we define

$$a_{1+}^{(i)}(z) = f_{0,M;-} \left(\frac{1}{z} \right) f_{0,M;+}(z) s_{1+}^{(i)}(z), \quad (4.15)$$

$$a_{1-}^{(i)}(z) = f_{0,M;+} \left(\frac{1}{z} \right) f_{0,M;-}(z) s_{1-}^{(i)}(z), \quad (4.16)$$

for $i = 1, 2$, we have

$$a_1(z) = a_{1+}^{(1)}(z) a_{1-}^{(1)}(z) = a_{1+}^{(2)}(z) a_{1-}^{(2)}(z). \quad (4.17)$$

Then it is confirmed that the inverse A_1^{-1} is given by

$$A_1^{-1} = \frac{1}{2} \left\{ T \left(\frac{1}{a_{1+}^{(1)}} \right) T \left(\frac{1}{a_{1-}^{(1)}} \right) + T \left(\frac{1}{a_{1+}^{(2)}} \right) T \left(\frac{1}{a_{1-}^{(2)}} \right) \right\}, \quad (4.18)$$

which is the substitute for (4.8).

Now one can compute the generating function,

$$\begin{aligned} & \sum_{i,j=1}^{\infty} z_1^{1-i} (A_1^{-1})_{i,j} z_2^{j-1} \\ &= \sum_{k=1}^{\infty} \frac{1}{2} \left\{ \sum_{i \in \mathbb{Z}} z_1^{-i+k} \widehat{\left(\frac{1}{a_{1+}^{(1)}} \right)}(i-k) \sum_{j \in \mathbb{Z}} \widehat{\left(\frac{1}{a_{1-}^{(1)}} \right)}(k-j) z_2^{j-k} \right. \\ & \quad \left. + \sum_{i \in \mathbb{Z}} z_1^{-i+k} \widehat{\left(\frac{1}{a_{1+}^{(2)}} \right)}(i-k) \sum_{j \in \mathbb{Z}} \widehat{\left(\frac{1}{a_{1-}^{(2)}} \right)}(k-j) z_2^{j-k} \right\} \left(\frac{z_2}{z_1} \right)^{k-1} \\ &= \frac{1}{1-z_2/z_1} \frac{1}{2} \left\{ \frac{1}{a_{1+}^{(1)}(\frac{1}{z_1}) a_{1-}^{(1)}(\frac{1}{z_2})} + \frac{1}{a_{1+}^{(2)}(\frac{1}{z_1}) a_{1-}^{(2)}(\frac{1}{z_2})} \right\} \\ &= \frac{z_1}{z_1 - z_2} \frac{1}{f_{0,M;-}(z_1) f_{0,M;+}(\frac{1}{z_1}) f_{0,M;+}(z_2) f_{0,M;-}(\frac{1}{z_2})} \\ & \quad \times \frac{1}{2} \left\{ \frac{1}{s_{1+}^{(1)}(\frac{1}{z_1}) s_{1-}^{(1)}(\frac{1}{z_2})} + \frac{1}{s_{1+}^{(2)}(\frac{1}{z_1}) s_{1-}^{(2)}(\frac{1}{z_2})} \right\}, \quad (4.19) \end{aligned}$$

which is valid for $|z_1| > |z_2|$. In the first equality we use a fact that $\widehat{\left(\frac{1}{a_{1+}^{(i)}} \right)}(k) = 0$ for $k < 0$ and $\widehat{\left(\frac{1}{a_{1-}^{(i)}} \right)}(k) = 0$ for $k > 0$ ($i = 1, 2$).

We also introduce the generating function of the function G_1 in (3.13). Note that as a function of x_1, x_2 , G_1 only depends on the difference $x_1 - x_2$, so that we can set

$$G_1(r_1, x_1; r_2, x_2) = (\hat{G}_1)_{r_1, r_2}(x_1 - x_2). \quad (4.20)$$

Then one has

$$(G_1)_{r_1, r_2}(z) = \sum_{k \in \mathbb{Z}} (\hat{G}_1)_{r_1, r_2}(k) z^k = f_{0, r_1}(z) s_1\left(\frac{1}{z}\right) f_{0, r_2}\left(\frac{1}{z}\right) = -f_{0, r_1}(z) s_1(z) f_{0, r_2}\left(\frac{1}{z}\right) \quad (4.21)$$

With these preparations, calculations of the generating functions of $\tilde{S}_1, \tilde{I}_1, D_1$ are not difficult. We have

$$\begin{aligned} \tilde{S}_1(r_1, z_1; r_2, z_2) &= \sum_{x_1, x_2 \in \mathbb{Z}} \tilde{S}_1(r_1, x_1; r_2, x_2) z_1^{x_1} z_2^{-x_2} \\ &= - \sum_{x_1, x_2} \sum_{i, j} \hat{f}_{r_1, M}(1 - i - x_1) z_1^{-1+i+x_1} \cdot z_1^{1-i} (A_1^{-1})_{i, j} z_2^{j-1} \cdot (\hat{G}_1)_{r_2, M}(x_2 - 1 + j) z_2^{-x_2+1-j} \\ &= -f_{r_1, M}\left(\frac{1}{z_1}\right) \cdot \sum_{i, j} z_1^{1-i} (A_1^{-1})_{i, j} z_2^{j-1} \cdot (G_1)_{r_2, M}\left(\frac{1}{z_2}\right) \\ &= \frac{z_1}{z_1 - z_2} \frac{f_{r_1, M; -}(\frac{1}{z_1}) f_{0, r_2; +}(\frac{1}{z_2}) f_{0, M; -}(z_2)}{f_{0, M; -}(z_1) f_{0, r_1; +}(\frac{1}{z_1}) f_{r_2, M; -}(\frac{1}{z_2})} \frac{1}{2} \left\{ \frac{s_{1+}^{(1)}(\frac{1}{z_2})}{s_{1+}^{(1)}(\frac{1}{z_1})} + \frac{s_{1+}^{(2)}(\frac{1}{z_2})}{s_{1+}^{(2)}(\frac{1}{z_1})} \right\}, \\ &= \frac{(1 - \alpha)^{2(u_2 - u_1)} (1 - \alpha/z_1)^{N+u_1} (1 - \alpha z_2)^{N-u_2}}{(1 - \alpha z_1)^{N-u_1} (1 - \alpha/z_2)^{N+u_2}} \frac{z_1}{z_1 - z_2} \left\{ 1 + \frac{z_1 - z_2}{(1 + z_1)(z_2 - 1)} \right\}, \quad (4.22) \end{aligned}$$

$$\begin{aligned} \tilde{I}_1(r_1, z_1; r_2, z_2) &= \sum_{x_1, x_2 \in \mathbb{Z}} \tilde{I}_1(r_1, x_1; r_2, x_2) z_1^{x_1} z_2^{-x_2} \\ &= -(G_1)_{r_1, M}(z_1) \cdot \sum_{i, j} z_1^{1-i} (A_1^{-1})_{i, j} z_2^{j-1} \cdot (G_1)_{r_2, M}\left(\frac{1}{z_2}\right) \\ &= \frac{z_1}{z_1 - z_2} \frac{f_{0, r_1; +}(z_1) f_{0, M; -}(\frac{1}{z_1}) f_{0, r_2; +}(\frac{1}{z_2}) f_{0, M; -}(z_2)}{f_{r_1, M; -}(z_1) f_{r_2, M; -}(\frac{1}{z_2})} \\ &\quad \times \frac{1}{2} \left\{ s_{1-}^{(1)}\left(\frac{1}{z_1}\right) s_{1+}^{(1)}\left(\frac{1}{z_2}\right) + s_{1-}^{(2)}\left(\frac{1}{z_1}\right) s_{1+}^{(2)}\left(\frac{1}{z_2}\right) \right\}, \\ &= \frac{(1 - \alpha)^{2(u_1 + u_2)} (1 - \alpha/z_1)^{N-u_1} (1 - \alpha z_2)^{N-u_2}}{(1 - \alpha z_1)^{N+u_1} (1 - \alpha/z_2)^{N+u_2}} \frac{z_1}{z_1 - z_2} \left\{ \frac{1}{2} \frac{z_2 + 1}{z_2 - 1} - \frac{1}{2} \frac{1 + z_1}{1 - z_1} \right\}, \quad (4.23) \end{aligned}$$

$$\begin{aligned}
\mathbb{D}_1(r_1, z_1; r_2, z_2) &= \sum_{x_1, x_2 \in \mathbb{Z}} D(r_1, x_1; r_2, x_2) z_1^{x_1} z_2^{-x_2} \\
&= -f_{r_1, M} \left(\frac{1}{z_1} \right) \cdot \sum_{i, j} z_1^{1-i} (A_1^{-1})_{i, j} z_2^{j-1} \cdot f_{r_2, M}(z_2) \\
&= \frac{z_1}{z_1 - z_2} \frac{f_{r_1, M; -}(\frac{1}{z_1}) f_{r_2, M; -}(z_2)}{f_{0, M; -}(z_1) f_{0, r_1; +}(\frac{1}{z_1}) f_{0, r_2; +}(z_2) f_{r_2, M; -}(\frac{1}{z_2})} \frac{1}{2} \left\{ \frac{1}{s_{1+}^{(1)}(\frac{1}{z_1}) s_{1-}^{(1)}(\frac{1}{z_2})} + \frac{1}{s_{1+}^{(2)}(\frac{1}{z_1}) s_{1-}^{(2)}(\frac{1}{z_2})} \right\} \\
&= \frac{(1 - \alpha/z_1)^{N+u_1} (1 - \alpha z_2)^{N+u_2}}{(1 - \alpha)^{2(u_1+u_2)} (1 - \alpha z_1)^{N-u_1} (1 - \alpha/z_2)^{N-u_2}} \frac{z_1}{z_1 - z_2} \left\{ \frac{1}{2} \frac{z_1 - 1}{z_1 + 1} - \frac{1}{2} \frac{1 - z_2}{1 + z_2} \right\}. \quad (4.24)
\end{aligned}$$

In the last expressions of these, we have set $r_i = 2u_i$ for $i = 1, 2$.

4.2 Bulk

We are now in a position to study the asymptotic behaviors of the model. The thermodynamic limit shape is already known to be

$$h(r = 2\beta_0 N, t = 2N)/N \sim \frac{2\alpha}{1 - \alpha^2} \left(\alpha + \sqrt{1 - \beta_0^2} \right), \quad (4.25)$$

where $0 < \beta_0 < 1$ is fixed [37]. As for the fluctuation around this limit shape, the KPZ theory tells us that the correlation survives for $O(N^{1/3})$ along the height direction and $O(N^{2/3})$ along the r direction.

Let us define the scaled height variable as

$$H_N(\tau, \beta_0) = \frac{h(r = 2\beta_0 N + 2c(\beta_0)N^{\frac{2}{3}}\tau, t = 2N) - a(\beta_0 + \frac{c(\beta_0)\tau}{N^{1/3}})N}{d(\beta_0)N^{\frac{1}{3}}}, \quad (4.26)$$

where

$$a(\beta) = \frac{2\alpha}{1 - \alpha^2} \left(\alpha + \sqrt{1 - \beta^2} \right), \quad (4.27)$$

$$d(\beta) = \frac{\alpha^{\frac{1}{3}}}{(1 - \alpha^2)(1 - \beta^2)^{\frac{1}{6}}} (\sqrt{1 + \beta} + \alpha\sqrt{1 - \beta})^{\frac{2}{3}} (\sqrt{1 - \beta} + \alpha\sqrt{1 + \beta})^{\frac{2}{3}}, \quad (4.28)$$

$$c(\beta) = \alpha^{-\frac{1}{3}} (1 - \beta^2)^{\frac{2}{3}} (\sqrt{1 + \beta} + \alpha\sqrt{1 - \beta})^{\frac{1}{3}} (\sqrt{1 - \beta} + \alpha\sqrt{1 + \beta})^{\frac{1}{3}}. \quad (4.29)$$

Remark that $a(\beta)$ just comes from the limit shape (4.25) whereas $d(\beta)$ and $c(\beta)$ are taken so that the results become simple. In this subsection, we show that the fluctuation of the model in the bulk is described by the Airy process [14, 19]. Namely, we show

Proposition 4.1.

$$\lim_{N \rightarrow \infty} \mathbb{P}[H_N(\tau_1, \beta_0) \leq s_1, \dots, H_N(\tau_m, \beta_0) \leq s_m] = \det(1 + \mathcal{K}_2 \mathcal{G}). \quad (4.30)$$

The determinant on the right hand side is the Fredholm determinant,

$$\det(1 + \mathcal{K}_2 \mathcal{G}) = \sum_{k=0}^{\infty} \frac{1}{k!} \sum_{\tau_1=1}^m \int d\xi_1 \cdots \sum_{\tau_k=1}^m \int d\xi_k \mathcal{G}(\tau_1, \xi_1) \cdots \mathcal{G}(\tau_k, \xi_k) \det(\mathcal{K}_2(\tau_l, \xi_l; \tau_{l'}, \xi_{l'}))_{l, l'=1}^k, \quad (4.31)$$

where $\mathcal{G}(\tau_j, \xi) = -\chi_{(s_j, \infty)}(x)$ ($j = 1, 2, \dots, m$) and \mathcal{K}_2 is a scalar kernel, for which a representative element is given by

$$\mathcal{K}_2(\tau_1, \xi_1; \tau_2, \xi_2) = \tilde{\mathcal{K}}_2(\tau_1, \xi_1; \tau_2, \xi_2) - \Phi_{\tau_1, \tau_2}(\xi_1, \xi_2), \quad (4.32)$$

with

$$\tilde{\mathcal{K}}_2(\tau_1, \xi_1; \tau_2, \xi_2) = \int_0^{\infty} d\lambda e^{-\lambda(\tau_1 - \tau_2)} \text{Ai}(\xi_1 + \lambda) \text{Ai}(\xi_2 + \lambda), \quad (4.33)$$

$$\Phi_{\tau_1, \tau_2}(\xi_1, \xi_2) = \begin{cases} 0, & \tau_1 \geq \tau_2, \\ \int_{-\infty}^{\infty} d\lambda e^{-\lambda(\tau_1 - \tau_2)} \text{Ai}(\xi_1 + \lambda) \text{Ai}(\xi_2 + \lambda), & \tau_1 < \tau_2. \end{cases} \quad (4.34)$$

Remark. The kernel (4.32) is called the extended Airy kernel and had already appeared in the context of Dyson's Brownian motion model [38, 39]. We also remark that some properties of the Airy process have been discussed in [14, 19, 40, 41]. For the special case of a single time, we have

$$\lim_{N \rightarrow \infty} \mathbb{P}[H_N(\tau, \beta_0) \leq \xi] = F_2(\xi), \quad (4.35)$$

where $F_2(\xi)$ is the GUE Tracy-Widom distribution [20]. In the language of the last passage percolation, (4.35) means that the fluctuation of the last passage time at an off-diagonal point is described by the GUE Tracy-Widom distribution. For the nonsymmetric case, the statement has been already established in [6]. But for our symmetric case, this has not seem to be shown although it was already expected based on a physical argument in [7]. Remember also that the fluctuation at an off-diagonal point has not been handled by the techniques using the Riemann-Hilbert method [25].

Proof. Let us derive (4.30). We first remark that (4.33) has a double contour integral representation,

$$\tilde{\mathcal{K}}_2(\tau_1, \xi_1; \tau_2, \xi_2) = -\frac{1}{4\pi^2} \int_{\text{Im} w_1 = \eta_1} d w_1 \int_{\text{Im} w_2 = \eta_2} d w_2 \frac{e^{i\xi_1 w_1 + i\xi_2 w_2 + \frac{i}{3}(w_1^3 + w_2^3)}}{\tau_2 - \tau_1 + i(w_1 + w_2)},$$

when $\eta_1 + \eta_2 + \tau_1 - \tau_2 > 0$, $\eta_1, \eta_2 > 0$, and that (4.34) can be computed as

$$\Phi_{\tau_1, \tau_2}(\xi_1, \xi_2) = \frac{1}{\sqrt{4\pi(\tau_2 - \tau_1)}} e^{-\frac{(\xi_2 - \xi_1)^2}{4(\tau_2 - \tau_1)} - \frac{1}{2}(\tau_2 - \tau_1)(\xi_1 + \xi_2) + \frac{1}{12}(\tau_2 - \tau_1)^3} \quad (4.36)$$

when $\tau_2 > \tau_1$. These are already given in [19].

Using the generating functions in the previous subsection, we get the double contour integral formula for $\tilde{S}_1, \tilde{I}_1, D_1$,

$$\tilde{S}_1(r_1, x_1; r_2, x_2) = \frac{1}{(2\pi i)^2} \int_{C_{R_1}} \frac{dz_1}{z_1^{x_1+1}} \int_{C_{R_2}} dz_2 z_2^{x_2-1} \tilde{S}_1(r_1, z_1; r_2, z_2), \quad (4.37)$$

$$\tilde{I}_1(r_1, x_1; r_2, x_2) = \frac{1}{(2\pi i)^2} \int_{C_{R_1}} \frac{dz_1}{z_1^{x_1+1}} \int_{C_{R_2}} dz_2 z_2^{x_2-1} \tilde{I}_1(r_1, z_1; r_2, z_2), \quad (4.38)$$

$$D_1(r_1, x_1; r_2, x_2) = \frac{1}{(2\pi i)^2} \int_{C_{R_1}} \frac{dz_1}{z_1^{x_1+1}} \int_{C_{R_2}} dz_2 z_2^{x_2-1} \mathbb{D}_1(r_1, z_1; r_2, z_2). \quad (4.39)$$

Here C_R denotes a contour enclosing the origin anticlockwise with radius R . We have taken $R_1 > R_2$ to agree with the computation in (4.19). For \tilde{I}_1 , exchanging the radius of the contours of z_1, z_2 gives

$$\begin{aligned} & \tilde{I}_1(r_1, x_1; r_2, x_2) \\ &= \frac{1}{(2\pi i)^2} \int_{C_{R_2}} \frac{dz_1}{z_1^{x_1+1}} \int_{C_{R_1}} dz_2 z_2^{x_2-1} \tilde{I}_1(r_1, z_1; r_2, z_2) - \frac{1}{2\pi i} \int_{C_{R_2}} dz_2 z_2^{x_2-x_1-1} (G_1)_{r_2, r_1} \left(\frac{1}{z_2} \right) \\ &= \frac{1}{(2\pi i)^2} \int_{C_{R_2}} \frac{dz_1}{z_1^{x_1+1}} \int_{C_{R_1}} dz_2 z_2^{x_2-1} \tilde{I}_1(r_1, z_1; r_2, z_2) + G_1(r_1, x_1; r_2, x_2). \end{aligned} \quad (4.40)$$

In the first equality the second term on the right hand side appears from the contribution of a pole at $z_1 = z_2$. Hence one gets the double contour integral representation for I_1 ,

$$I_1(r_1, x_1; r_2, x_2) = \frac{1}{(2\pi i)^2} \int_{C_{R_2}} \frac{dz_1}{z_1^{x_1+1}} \int_{C_{R_1}} dz_2 z_2^{x_2-1} \tilde{I}_1(r_1, z_1; r_2, z_2). \quad (4.41)$$

Let us first consider the asymptotics of \tilde{S}_1 . Since we can follow the discussions in [19] for a large part, we omit details and state the main steps. If we write

$$g_{\mu, \beta}(z) = (1 + \beta) \log(z - \alpha) - (1 - \beta) \log(1 - \alpha z) - (\mu + \beta) \log z, \quad (4.42)$$

we have

$$\begin{aligned} & \tilde{S}_1(r_1 = 2u_1, x_1; r_2 = 2u_2, x_2) \\ &= \frac{(1 - \alpha)^{2(u_2 - u_1)}}{(2\pi i)^2} \int_{C_{R_1}} \frac{dz_1}{z_1} \int_{C_{R_2}} \frac{dz_2}{z_2} \frac{z_2^{x_2 - N(\mu_2 - 1)}}{z_1^{x_1 - N(\mu_1 - 1)}} e^{N(g_{\mu_1, \beta_1}(z_1) + g_{\mu_2, \beta_2}(1/z_2))} \\ & \quad \times \frac{z_1}{z_1 - z_2} \left\{ 1 + \frac{z_1 - z_2}{(1 + z_1)(z_2 - 1)} \right\}, \end{aligned} \quad (4.43)$$

where $\beta_1 = u_1/N, \beta_2 = -u_2/N$. μ_1, μ_2 are arbitrary constants at this stage. We would like to apply the saddle point method to this integral. In general for each value of μ , there are

two critical points $z_c^\pm = p(\mu, \beta) \pm \sqrt{p(\mu, \beta)^2 - q(\mu, \beta)}$ with

$$p(\mu, \beta) = \frac{\mu(1 + \alpha^2) - (1 - \alpha^2)}{2\alpha(\mu - \beta)}, \quad (4.44)$$

$$q(\mu, \beta) = \frac{\mu + \beta}{\mu - \beta}. \quad (4.45)$$

Since we are considering the scaling in (4.26), we will set

$$x_i = Na(\beta_i) + d(\beta_0)N^{\frac{1}{3}}\xi_i, \quad (4.46)$$

with ξ_i the scaled space variable. Accordingly we set $\mu_i = \mu_c(\beta_i)$ with

$$\mu_c(\beta) = a(\beta) + 1 = \frac{1}{1 - \alpha^2} \left(1 + \alpha^2 + 2\alpha\sqrt{1 - \beta^2} \right). \quad (4.47)$$

For this special value of μ , the two critical points, z_c^\pm , merge to the double critical point $p_c(\beta)$, where $g'_{\mu_c(\beta), \beta}(p_c(\beta)) = g''_{\mu_c(\beta), \beta}(p_c(\beta)) = 0$, given by

$$p_c(\beta) = p(\mu_c(\beta), \beta) = \frac{\sqrt{1 + \beta} + \alpha\sqrt{1 - \beta}}{\sqrt{1 - \beta} + \alpha\sqrt{1 + \beta}}. \quad (4.48)$$

The main contribution to the integral in (4.43) comes from around the double critical points $z_1 \sim p_c(\beta_1)$, $z_2 \sim 1/p_c(\beta_2)$. The paths of integration may be deformed to

$$z_1 = p_c(\beta_1) \left(1 - \frac{i}{d(\beta_0)N^{1/3}}w_1 \right), \quad (4.49)$$

$$\frac{1}{z_2} = p_c(\beta_2) \left(1 - \frac{i}{d(\beta_0)N^{1/3}}w_2 \right), \quad (4.50)$$

where $w_i = \zeta_i + i\eta_i$ with $-\infty < \zeta_i < \infty$ ($i = 1, 2$) and $\eta_1, \eta_2 > 0$ are fixed. For a fixed β_0 , we take

$$r_i = 2u_i = 2N \left(\beta_0 + \frac{c(\beta_0)\tau_i}{N^{1/3}} \right), \quad (4.51)$$

where τ_i is the scaled time variable. To leading order we have

$$p_c(\beta_1) = p_c(\beta_0) + p'_c(\beta_0)(\beta_1 - \beta_0) = p_c(\beta_0) \left(1 + \frac{\tau_1}{d(\beta_0)N^{1/3}} \right), \quad (4.52)$$

$$p_c(\beta_2) = p_c(-\beta_0) + p'_c(-\beta_0)(\beta_2 + \beta_0) = p_c(-\beta_0) \left(1 - \frac{\tau_2}{d(\beta_0)N^{1/3}} \right), \quad (4.53)$$

where

$$c(\beta_0) = \frac{p_c(\beta_0)}{p'_c(\beta_0)d(\beta_0)} = \frac{p_c(-\beta_0)}{p'_c(-\beta_0)d(\beta_0)} \quad (4.54)$$

is used.

Expanding around $z_1 \sim p_c(\beta_1)$ to order $O(1)$, one finds

$$\begin{aligned}
Ng_{\mu_c(\beta_1),\beta_1}(z_1) &\sim Ng_{\mu_c(\beta_1),\beta_1}(p_c(\beta_1)) + \frac{1}{6}g_{\mu_c(\beta_1),\beta_1}'''(p_c(\beta_1)) \left(-i\frac{p_c(\beta_1)}{d(\beta_0)}w_1\right)^3 \\
&\sim Ng_{\mu_c(\beta_1),\beta_1}(p_c(\beta_1)) + \frac{i}{3}\frac{p_c(\beta_0)^3}{2d(\beta_0)^3}g_{\mu_c(\beta_0),\beta_0}'''(p_c(\beta_0))w_1^3 \\
&= Ng_{\mu_c(\beta_1),\beta_1}(p_c(\beta_1)) + \frac{i}{3}w_1^3
\end{aligned} \tag{4.55}$$

after some computation. Similarly one gets

$$Ng_{\mu_c(\beta_2),\beta_2}(1/z_2) \sim Ng_{\mu_c(\beta_2),\beta_2}(p_c(\beta_2)) + \frac{i}{3}w_2^3. \tag{4.56}$$

Let us denote

$$\begin{aligned}
\lambda_0(\beta) &= g_{\mu_c(\beta),\beta}(p_c(\beta)) \\
&= 2\beta \log(1 - \alpha^2) + \frac{1}{2}(1 + \beta) \log(1 + \beta) - \frac{1}{2}(1 - \beta) \log(1 - \beta) \\
&\quad + \frac{1}{1 - \alpha^2}(\sqrt{1 - \beta} + \alpha\sqrt{1 + \beta})^2 \log(\sqrt{1 - \beta} + \alpha\sqrt{1 + \beta}) \\
&\quad - \frac{1}{1 - \alpha^2}(\sqrt{1 + \beta} + \alpha\sqrt{1 - \beta})^2 \log(\sqrt{1 + \beta} + \alpha\sqrt{1 - \beta}).
\end{aligned} \tag{4.57}$$

Clearly, this is an odd function. Therefore if we expand as

$$\lambda(\beta) \sim \lambda_0(\beta_0) + \lambda_1(\beta_0)(\beta - \beta_0) + \lambda_2(\beta_0)(\beta - \beta_0)^2 + \lambda_3(\beta_0)(\beta - \beta_0)^3 + \dots \tag{4.58}$$

we have $\lambda_i(\beta_0) = (-1)^{i+1}\lambda_i(-\beta_0)$ for $i = 0, 1, 2, \dots$. Expanding to order $O(1)$, we have

$$\begin{aligned}
Ng_{\mu_c(\beta_1),\beta_1}(p_c(\beta_1)) &\sim N\lambda_0(\beta_0) + \lambda_1(\beta_0)c(\beta_0)N^{2/3}\tau_1 \\
&\quad + \lambda_2(\beta_0)c(\beta_0)^2N^{1/3}\tau_1^2 + \lambda_3(\beta_0)c(\beta_0)^3\tau_1^3,
\end{aligned} \tag{4.59}$$

$$\begin{aligned}
Ng_{\mu_c(\beta_2),\beta_2}(p_c(\beta_2)) &\sim -N\lambda_0(\beta_0) - \lambda_1(\beta_0)c(\beta_0)N^{2/3}\tau_2 \\
&\quad - \lambda_2(\beta_0)c(\beta_0)^2N^{1/3}\tau_2^2 - \lambda_3(\beta_0)c(\beta_0)^3\tau_2^3.
\end{aligned} \tag{4.60}$$

Combining (4.49),(4.50) with (4.52),(4.53) gives

$$z_1 = p_c(\beta_0) \left(1 + \frac{1}{d(\beta_0)N^{1/3}}(\tau_1 - iw_1)\right), \tag{4.61}$$

$$\frac{1}{z_2} = p_c(-\beta_0) \left(1 - \frac{1}{d(\beta_0)N^{1/3}}(\tau_2 + iw_2)\right), \tag{4.62}$$

so that

$$\frac{z_2^{x_2+N(1-\mu_c(\beta_2))}}{z_1^{x_1+N(1-\mu_c(\beta_1))}} \sim (p_c(\beta_0))^{(\xi_2-\xi_1)d(\beta_0)N^{1/3}} e^{\xi_2\tau_2-\xi_1\tau_1+i\xi_1w_1+i\xi_2w_2}. \tag{4.63}$$

In addition, to leading order we have

$$\frac{z_1}{z_1 - z_2} \left\{ 1 + \frac{z_1 - z_2}{(1 + z_1)(z_2 - 1)} \right\} \sim -\frac{d(\beta_0)N^{1/3}}{\tau_2 - \tau_1 + i(w_1 + w_2)}, \quad (4.64)$$

to which the second term on the left hand side does not contribute.

Finally one obtains

$$\begin{aligned} \tilde{S}_1 &\sim (1 - \alpha)^{2(u_2 - u_1)} (p_c(\beta_0))^{(\xi_2 - \xi_1)d(\beta_0)N^{1/3}} \frac{1}{d(\beta_0)N^{1/3}} \\ &\quad e^{\lambda_1(\beta_0)c(\beta_0)N^{2/3}(\tau_1 - \tau_2) + \lambda_2(\beta_0)c(\beta_0)^2N^{1/3}(\tau_1^2 - \tau_2^2) + \lambda_3(\beta_0)c(\beta_0)^3(\tau_1^3 - \tau_2^3) + \xi_2\tau_2 - \xi_1\tau_1} \\ &\quad \frac{1}{4\pi^2} \int_{\text{Im}w_1 = \eta_1} dw_1 \int_{\text{Im}w_2 = \eta_2} dw_2 \left(-\frac{1}{\tau_2 - \tau_1 + i(w_1 + w_2)} \right) e^{i\xi_1 w_1 + i\xi_2 w_2 + \frac{i}{3}(w_1^3 + w_2^3)}. \end{aligned} \quad (4.65)$$

We also need the asymptotics of

$$\begin{aligned} &\phi_{r_1, r_2}(x_1, x_2) \\ &= \frac{(1 - \alpha)^{2(u_2 - u_1)}}{2\pi i} \int_{C_1} \frac{dz}{z} z^{x_2 - x_1} [(1 - \alpha z)(1 - \alpha/z)]^{u_2 - u_1} \\ &= \frac{(1 - \alpha)^{2(u_2 - u_1)}}{2\pi i} \int_{C_1} \frac{dz}{z} z^{x_2 - N(\mu_c(\beta_2) - 1) - x_1 + N(\mu_c(\beta_1) - 1)} e^{Ng_{\mu_c(\beta_1), \beta_1}(z) + Ng_{\mu_c(\beta_2), \beta_2}(1/z)}. \end{aligned} \quad (4.66)$$

Let us set

$$z = p_c(\beta_0) \left(1 + \frac{i\sigma}{d(\beta_0)N^{1/3}} \right). \quad (4.67)$$

From (4.52), this can be rewritten as

$$z \sim p_c(\beta_1) \left(1 - \frac{1}{d(\beta_0)N^{1/3}}(\tau_1 - i\sigma) \right). \quad (4.68)$$

Expansion around $z \sim p_c(\beta_1)$ as in (4.55) gives

$$Ng_{\mu_c(\beta_1), \beta_1}(z) \sim Ng_{\mu_c(\beta_1), \beta_1}(p_c(\beta_1)) - \frac{1}{3}(\tau_1 - i\sigma)^3. \quad (4.69)$$

Similarly

$$\frac{1}{z} \sim p_c(\beta_2) \left(1 + \frac{1}{d(\beta_0)N^{1/3}}(\tau_2 - i\sigma) \right) \quad (4.70)$$

leads to

$$Ng_{\mu_c(\beta_2), \beta_2}\left(\frac{1}{z}\right) \sim Ng_{\mu_c(\beta_2), \beta_2}(p_c(\beta_2)) + \frac{1}{3}(\tau_2 - i\sigma)^3. \quad (4.71)$$

One also finds

$$z^{x_2 - N(\mu_c(\beta_2) - 1) - x_1 + N(\mu_c(\beta_1) - 1)} \sim (p_c(\beta_0))^{d(\beta_0)N^{1/3}(\xi_2 - \xi_1)} e^{i\sigma(\xi_2 - \xi_1)}. \quad (4.72)$$

Hence one gets

$$\begin{aligned}
\phi_{r_1, r_2}(x_1, x_2) &\sim (1 - \alpha)^{2(u_2 - u_1)} (p_c(\beta_0))^{(\xi_2 - \xi_1)d(\beta_0)N^{1/3}} \frac{1}{d(\beta_0)N^{1/3}} \\
&\quad e^{\lambda_1(\beta_0)c(\beta_0)N^{2/3}(\tau_1 - \tau_2) + \lambda_2(\beta_0)c(\beta_0)^2N^{1/3}(\tau_1^2 - \tau_2^2) + \lambda_3(\beta_0)c(\beta_0)^3(\tau_1^3 - \tau_2^3) - \frac{\tau_1^3}{3} + \frac{\tau_2^3}{3}} \\
&\quad \frac{1}{2\pi} \int_{-\infty}^{\infty} d\sigma e^{i(\xi_2 - \xi_1 + \tau_1^2 - \tau_2^2)\sigma - (\tau_2 - \tau_1)\sigma^2}. \tag{4.73}
\end{aligned}$$

For I_1 , one has

$$\begin{aligned}
&I_1(r_1 = 2u_1, x_1; r_2 = 2u_2, x_2) \\
&= \frac{(1 - \alpha)^{2(u_1 + u_2)}}{(2\pi i)^2} \int_{C_{R_2}} \frac{dz_1}{z_1} \int_{C_{R_1}} \frac{dz_2}{z_2} \frac{z_2^{x_2 - N(\mu_c(\beta_2) - 1)}}{z_1^{x_1 - N(\mu_c(\beta_1) - 1)}} e^{N(g_{\mu_c(\beta_1), \beta_1}(z_1) + g_{\mu_c(\beta_2), \beta_2}(1/z_2))} \\
&\quad \times \frac{z_1}{z_1 - z_2} \left\{ \frac{1}{2} \frac{z_2 + 1}{z_2 - 1} - \frac{1}{2} \frac{1 + z_1}{1 - z_1} \right\}, \tag{4.74}
\end{aligned}$$

where $\beta_i = -u_i/N$. The critical points of z_1, z_2 are the again given by $z_1 = p_c(\beta_1), z_2 = 1/p_c(\beta_2)$. To leading order, the paths are

$$z_1 = p_c(-\beta_0) \left(1 - \frac{1}{d(\beta_0)N^{1/3}}(\tau_1 + iw_1) \right), \tag{4.75}$$

$$\frac{1}{z_2} = p_c(-\beta_0) \left(1 - \frac{1}{d(\beta_0)N^{1/3}}(\tau_2 + iw_2) \right), \tag{4.76}$$

so that we have

$$\begin{aligned}
I_1 &\sim (1 - \alpha)^{2(u_1 + u_2)} \frac{p_c(-\beta_0)^3}{(1 + p_c(-\beta_0))(1 - p_c(-\beta_0))^3} (p_c(\beta_0))^{(\xi_1 + \xi_2)d(\beta_0)N^{1/3}} \frac{1}{d(\beta_0)^3 N} \\
&\quad e^{-2N\lambda_0(\beta_0) - \lambda_1(\beta_0)c(\beta_0)N^{2/3}(\tau_1 + \tau_2) - \lambda_2(\beta_0)c(\beta_0)^2N^{1/3}(\tau_1^2 + \tau_2^2) - \lambda_3(\beta_0)c(\beta_0)^3(\tau_1^3 + \tau_2^3) + \xi_1\tau_1 + \xi_2\tau_2} \\
&\quad \frac{1}{4\pi^2} \int_{\text{Im}w_1 = \eta_1} dw_1 \int_{\text{Im}w_2 = \eta_2} dw_2 (\tau_1 - \tau_2 + i(w_1 - w_2)) e^{i\xi_1 w_1 + i\xi_2 w_2 + \frac{i}{3}(w_1^3 + w_2^3)}. \tag{4.77}
\end{aligned}$$

Similarly for D_1 one has

$$\begin{aligned}
&D_1(r_1 = 2u_1, x_1; r_2 = 2u_2, x_2) \\
&= \frac{1}{(2\pi i)^2 (1 - \alpha)^{2(u_1 + u_2)}} \int_{C_{R_1}} \frac{dz_1}{z_1} \int_{C_{R_2}} \frac{dz_2}{z_2} \frac{z_2^{x_2 - N(\mu_c(\beta_2) - 1)}}{z_1^{x_1 - N(\mu_c(\beta_1) - 1)}} e^{N(g_{\mu_c(\beta_1), \beta_1}(z_1) + g_{\mu_c(\beta_2), \beta_2}(1/z_2))} \\
&\quad \times \frac{z_1}{z_1 - z_2} \left\{ \frac{1}{2} \frac{z_1 - 1}{z_1 + 1} - \frac{1}{2} \frac{1 - z_2}{1 + z_2} \right\}, \tag{4.78}
\end{aligned}$$

where $\beta_i = u_i/N$. The critical points of z_1, z_2 are $z_1 = p_c(\beta_1), z_2 = 1/p_c(\beta_2)$. To leading order, the paths are

$$z_1 = p_c(\beta_0) \left(1 + \frac{1}{d(\beta_0)N^{1/3}}(\tau_1 - iw_1) \right), \quad (4.79)$$

$$\frac{1}{z_2} = p_c(\beta_0) \left(1 + \frac{1}{d(\beta_0)N^{1/3}}(\tau_2 - iw_2) \right), \quad (4.80)$$

so that we have

$$D_1 \sim (1 - \alpha)^{-2(u_1+u_2)} \frac{p_c(\beta_0)}{(1 + p_c(\beta_0))(1 - p_c(\beta_0))^3} (p_c(\beta_0))^{-(\xi_1+\xi_2)d(\beta_0)N^{1/3}} \frac{1}{d(\beta_0)^3 N} e^{2N\lambda_0(\beta_0)+\lambda_1(\beta_0)c(\beta_0)N^{2/3}(\tau_1+\tau_2)+\lambda_2(\beta_0)c(\beta_0)^2N^{1/3}(\tau_1^2+\tau_2^2)+\lambda_3(\beta_0)c(\beta_0)^3(\tau_1^3+\tau_2^3)-\xi_1\tau_1-\xi_2\tau_2} \frac{1}{4\pi^2} \int_{\text{Im}w_1=\eta_1} dw_1 \int_{\text{Im}w_2=\eta_2} dw_2 (\tau_1 - \tau_2 - i(w_1 - w_2)) e^{i\xi_1w_1+i\xi_2w_2+\frac{i}{3}(w_1^3+w_2^3)}. \quad (4.81)$$

Now suppose that we substitute the asymptotic expressions (4.65),(4.73),(4.77),(4.81) into (3.6). Notice that the kernel of the form $\begin{bmatrix} a & b \\ c & d \end{bmatrix}$ and $\begin{bmatrix} \alpha a & \beta b \\ c/\beta & d/\alpha \end{bmatrix}$ give the same value for the determinant and hence that some of the prefactors in (4.65),(4.73), (4.77),(4.81) have no effect on the value of the determinant. Moreover, in our scaling limit, the off-diagonal elements, I_1 and D_1 , vanish due to the difference of order in N . The diagonal elements are transpose to each other and hence one finds

$$\begin{aligned} \mathbb{P}[h(r_1, 2N) \leq X_1, \dots, h(r_m, 2N) \leq X_m] &= \sqrt{\det(1 + K_1 g)} \\ \rightarrow \sqrt{(\det(1 + \mathcal{K}_2 \mathcal{G}))^2} &= \det(1 + \mathcal{K}_2 \mathcal{G}), \end{aligned} \quad (4.82)$$

where g is $g(r_i, x) = -\chi_{J_i}(x)$ ($i = 1, 2, \dots, m$), where $J_i = (X_i, \infty)$ and $r_i = 2\beta_0 N + 2c(\beta_0)N^{2/3}\tau_i$, $X_i = a(\beta_0 + \frac{c(\beta_0)\tau_i}{N^{1/3}})N + s_i d(\beta_0)N^{1/3}$ for $i = 1, 2, \dots, m$. \square

4.3 Near the Origin

In the last subsection, we saw that the fluctuation in the bulk is described by the Airy process. On the other hand, as already mentioned, we know that the height fluctuation at the origin is given by the GOE Tracy-Widom distribution. In this subsection, we are interested in the crossover between them. Let us define the scaled height variable near the origin as

$$H_N(\tau) = \frac{h(r = 2cN^{2/3}\tau, t = M = 2N) - aN}{dN^{1/3}} + \tau^2, \quad (4.83)$$

where

$$a = a(0) = \frac{2\alpha}{1-\alpha}, \quad (4.84)$$

$$d = d(0) = \frac{\alpha^{1/3}(1+\alpha)^{1/3}}{1-\alpha}, \quad (4.85)$$

$$c = c(0) = \frac{(1+\alpha)^{\frac{2}{3}}}{\alpha^{\frac{1}{3}}}. \quad (4.86)$$

The second term in (4.83) comes from the expansion of $a(\beta)$ in (4.27) around $\beta = 0$.

We show that the fluctuation of the model near the origin is described by the process which gives the orthogonal-unitary transition in random matrix theory. Namely, we show

Theorem 4.2.

$$\lim_{N \rightarrow \infty} \mathbb{P}[H_N(\tau_1) \leq s_1, \dots, H_N(\tau_m) \leq s_m] = \sqrt{\det(1 + \mathcal{K}_1 \mathcal{G})}, \quad (4.87)$$

where $\mathcal{G}(\tau_j, \xi) = -\chi_{(s_j, \infty)}(\xi)$ ($j = 1, 2, \dots, m$) and \mathcal{K}_1 is the 2×2 matrix kernel, for which a representative element is given by

$$\mathcal{K}_1(\tau_1, \xi_1; \tau_2, \xi_2) = \begin{bmatrix} \mathcal{S}_1(\tau_1, \xi_1; \tau_2, \xi_2) & \mathcal{D}_1(\tau_1, \xi_1; \tau_2, \xi_2) \\ \mathcal{I}_1(\tau_1, \xi_1; \tau_2, \xi_2) & \mathcal{S}_1(\tau_2, \xi_2; \tau_1, \xi_1) \end{bmatrix}, \quad (4.88)$$

with the matrix elements being

$$\mathcal{S}_1(\tau_1, \xi_1; \tau_2, \xi_2) = \tilde{\mathcal{S}}_1(\tau_1, \xi_1; \tau_2, \xi_2) - \Phi_{\tau_1, \tau_2}(\xi_1, \xi_2), \quad (4.89)$$

$$\tilde{\mathcal{S}}_1(\tau_1, \xi_1; \tau_2, \xi_2) = \int_0^\infty d\lambda e^{-\lambda(\tau_1 - \tau_2)} \text{Ai}(\xi_1 + \lambda) \text{Ai}(\xi_2 + \lambda) + \frac{1}{2} \text{Ai}(\xi_1) \int_0^\infty d\lambda e^{-\lambda\tau_2} \text{Ai}(\xi_2 - \lambda), \quad (4.90)$$

$$\begin{aligned} \mathcal{I}_1(\tau_1, \xi_1; \tau_2, \xi_2) &= - \int_0^\infty d\lambda e^{-\lambda\tau_1} \text{Ai}(\xi_1 - \lambda) \int_\lambda^\infty d\nu e^{-\nu\tau_2} \text{Ai}(\xi_2 - \nu) \\ &\quad + \int_0^\infty d\lambda e^{-\lambda\tau_2} \text{Ai}(\xi_2 - \lambda) \int_\lambda^\infty d\nu e^{-\nu\tau_1} \text{Ai}(\xi_1 - \nu), \end{aligned} \quad (4.91)$$

$$\begin{aligned} \mathcal{D}_1(\tau_1, \xi_1; \tau_2, \xi_2) &= -\frac{1}{4} \int_0^\infty d\lambda e^{-\lambda\tau_2} \text{Ai}(\xi_2 + \lambda) \frac{d}{d\lambda} \{e^{-\lambda\tau_1} \text{Ai}(\xi_1 + \lambda)\} \\ &\quad + \frac{1}{4} \int_0^\infty d\lambda e^{-\lambda\tau_1} \text{Ai}(\xi_1 + \lambda) \frac{d}{d\lambda} \{e^{-\lambda\tau_2} \text{Ai}(\xi_2 + \lambda)\}. \end{aligned} \quad (4.92)$$

Definition of $\Phi_{\tau_1, \tau_2}(\xi_1, \xi_2)$ is already given in (4.34).

Remark. The same kernel appeared in the context of the orthogonal-unitary transition in [28] and the problem of vicious walks in [33]. For the special case of a fluctuation at $\tau = 0$, we have

$$\lim_{N \rightarrow \infty} \mathbb{P}[H_N(0) \leq s] = F_1(s), \quad (4.93)$$

where $F_1(s)$ is the GOE Tracy-Widom distribution [22]. It is remarked that this result was anticipated in [6] based on the Meixner orthogonal ensemble representation and was shown in [25]. On the other hand, for $\tau \rightarrow \infty$, \mathcal{I}_1 and \mathcal{D}_1 goes to zero. We recover the Airy process, which is consistent with the results of the previous subsection.

Proof. Let us derive (4.87). We first notice that (4.90), (4.91), (4.92) have double contour integral representation. Assume $\tau_1, \tau_2 \geq 0$ and $\eta_1, \eta_2 > 0$. For $\tilde{\mathcal{S}}_1$, one has

$$\begin{aligned} & \tilde{\mathcal{S}}_1(\tau_1, \xi_1; \tau_2, \xi_2) \\ &= \frac{1}{4\pi^2} \int_{\text{Im}w_1=\eta_1} dw_1 \int_{\text{Im}w_2=\eta_2} dw_2 \left(-\frac{1}{\tau_2 - \tau_1 + i(w_1 + w_2)} + \frac{1}{2(\tau_2 + iw_2)} \right) \\ & \quad e^{i\xi_1 w_1 + i\xi_2 w_2 + \frac{i}{3}(w_1^3 + w_2^3)}, \end{aligned} \quad (4.94)$$

where $\eta_1 + \eta_2 + \tau_1 - \tau_2 > 0$ and $\tau_2 - \eta_2 > 0$. For \mathcal{I}_1 ,

$$\begin{aligned} & \mathcal{I}_1(\tau_1, \xi_1; \tau_2, \xi_2) \\ &= \frac{1}{4\pi^2} \int_{\text{Im}w_1=\eta_1} dw_1 \int_{\text{Im}w_2=\eta_2} dw_2 \frac{-1}{(\tau_2 + iw_2)(\tau_1 + \tau_2 + i(w_1 + w_2))} e^{i\xi_1 w_1 + i\xi_2 w_2 + \frac{i}{3}(w_1^3 + w_2^3)} \\ & \quad - (\tau_1, \xi_1 \leftrightarrow \tau_2, \xi_2), \end{aligned} \quad (4.95)$$

where $\tau_1 - \eta_1 > 0, \tau_2 - \eta_2 > 0$. For \mathcal{D}_1 ,

$$\begin{aligned} & \mathcal{D}_1(\tau_1, \xi_1; \tau_2, \xi_2) \\ &= \frac{1}{4\pi^2} \int_{\text{Im}w_1=\eta_1} dw_1 \int_{\text{Im}w_2=\eta_2} dw_2 \frac{\tau_1 - iw_1}{4(\tau_1 + \tau_2 - i(w_1 + w_2))} e^{i\xi_1 w_1 + i\xi_2 w_2 + \frac{i}{3}(w_1^3 + w_2^3)} \\ & \quad - (\tau_1, \xi_1 \leftrightarrow \tau_2, \xi_2), \end{aligned} \quad (4.96)$$

where there is no additional condition on $\tau_1, \tau_2, \eta_1, \eta_2$. These are easily obtained by using the integral representation of the Airy function,

$$\text{Ai}(\xi) = \frac{1}{2\pi} \int_{\text{Im} w=\eta} dw e^{i\xi w + i\frac{w^3}{3}}. \quad (4.97)$$

In the following, we show, as $N \rightarrow \infty$,

$$S_1(r_1, x_1; r_2, x_2) \sim e^{(\tau_1^3 - \tau_2^3)/3 - \xi_1 \tau_1 + \xi_2 \tau_2} dN^{1/3} \mathcal{S}_1(\tau_1, \xi_1; \tau_2, \xi_2), \quad (4.98)$$

$$I_1(r_1, x_1; r_2, x_2) \sim e^{-(\tau_1^3 + \tau_2^3)/3 + \xi_1 \tau_1 + \xi_2 \tau_2} \mathcal{I}_1(\tau_1, \xi_1; \tau_2, \xi_2), \quad (4.99)$$

$$D_1(r_1, x_1; r_2, x_2) \sim e^{(\tau_1^3 + \tau_2^3)/3 - \xi_1 \tau_1 - \xi_2 \tau_2} d^2 N^{2/3} \mathcal{D}_1(\tau_1, \xi_1; \tau_2, \xi_2), \quad (4.100)$$

where we set $r_i = 2cN^{2/3}\tau_i, x_i = aN + (\xi_i - \tau_i^2)dN^{1/3}$ for $i = 1, 2$. From these, (4.87) is almost obvious.

Let us first consider the asymptotics of $\tilde{\mathcal{S}}_1$. Basically one can follow the same route as in the last subsection with $\beta_0 = 0$, but there appear some simplifications and differences. For instance, (4.61),(4.62) reduce to

$$z_1 = 1 + \frac{1}{dN^{1/3}}(\tau_1 - iw_1), \quad \frac{1}{z_2} = 1 - \frac{1}{dN^{1/3}}(\tau_2 + iw_2). \quad (4.101)$$

Then we have

$$\frac{z_1}{z_1 - z_2} \left\{ 1 + \frac{z_1 - z_2}{(1 + z_1)(z_2 - 1)} \right\} \sim -\frac{dN^{1/3}}{\tau_2 - \tau_1 + i(w_1 + w_2)} + \frac{1}{2} \frac{dN^{1/3}}{\tau_2 + iw_2}. \quad (4.102)$$

Compare this with (4.64), where the second term on the left hand side was negligible.

Expansion of $G(\beta)$ in (4.58) is now simply

$$G(\beta) = 2 \log(1 - \alpha) \beta + \frac{\alpha}{3(1 + \alpha)^2} \beta^3, \quad (4.103)$$

so that one has

$$e^{Ng_{\mu_c(\beta_1), \beta_1}(p_c(\beta_1))} \sim (1 - \alpha)^{2u_1} e^{\tau_1^3/3}, \quad (4.104)$$

$$e^{Ng_{\mu_c(\beta_2), \beta_2}(p_c(\beta_2))} \sim (1 - \alpha)^{-2u_2} e^{-\tau_2^3/3}, \quad (4.105)$$

instead of (4.59),(4.60). Asymptotics of ϕ , which is already given in [19], can be obtained by setting $\beta_0 = 0$ in (4.73);

$$\phi_{r_1, r_2}(x_1, x_2) = e^{(\tau_2^3 - \tau_1^3)/3 + \xi_1 \tau_1 - \xi_2 \tau_2} dN^{1/3} \Phi_{\tau_1, \tau_2}(\xi_1, \xi_2). \quad (4.106)$$

Combining these, we see (4.98) holds.

As for I_1 , (4.75),(4.76) reduce to

$$z_1 = 1 - \frac{1}{dN^{1/3}}(\tau_1 + iw_1), \quad \frac{1}{z_2} = 1 - \frac{1}{dN^{1/3}}(\tau_2 + iw_2). \quad (4.107)$$

Since

$$\frac{z_1}{z_1 - z_2} \left\{ \frac{1}{2} \frac{z_2 + 1}{z_2 - 1} - \frac{1}{2} \frac{1 + z_1}{1 - z_1} \right\} \sim \frac{d^2 N^{2/3}}{\tau_1 + \tau_2 + i(w_1 + w_2)} \left(\frac{-1}{\tau_2 + iw_2} - \frac{-1}{\tau_1 + iw_1} \right), \quad (4.108)$$

we see that (4.99) holds.

Finally, for D_1 , (4.79),(4.80) reduce to

$$z_1 = 1 + \frac{1}{dN^{1/3}}(\tau_1 - iw_1), \quad \frac{1}{z_2} = 1 + \frac{1}{dN^{1/3}}(\tau_2 - iw_2). \quad (4.109)$$

Since

$$\frac{z_1}{z_1 - z_2} \left\{ \frac{1}{2} \frac{z_1 - 1}{z_1 + 1} - \frac{1}{2} \frac{1 - z_2}{1 + z_2} \right\} \sim \frac{1}{4} \frac{(\tau_1 - iw_1) - (\tau_2 - iw_2)}{\tau_1 + \tau_2 - i(w_1 + w_2)}, \quad (4.110)$$

we see that (4.100) holds. \square

5 Model without Source at the Origin

In this section we study the case where $\gamma = 0$ in (2.4). As already mentioned in the introduction, this case corresponds to the PNG model without the source at the origin. The analysis proceeds in a fairly parallel way to the orthogonal case. The main difference is that there is a new restriction on the height lines h_i ; $h_{2i}(0, t) = h_{2i+1}(0, t) + 1$ ($i = 0, 1, \dots, N/2 - 1$) at time $t = M = 2N$. Here and hereafter we assume N is even. This condition might look somewhat strange at first sight, but in fact can be understood after a short reflection. An example of a multi-layer heights is given in Fig. 3, in which one sees that h_{2i} and h_{2i+1} form a pair at $r = 0$. As in the orthogonal case, we change the way of looking at multi-layer heights. The space coordinate r will be interpreted as the time coordinate. The height coordinate will be interpreted as the space coordinate and is represented as x . Then the restrictions read $x_i^M = 1 - i$ for $i = 1, 2, \dots, N$ and $x_{2i}^0 = x_{2i-1}^0 - 1$ for $i = 1, 2, \dots, N/2$.

5.1 Determinantal Process and Kernel

We consider the weight of non-intersecting paths of n particles given by

$$w_{n,M}(\bar{x}) = \det \left(\begin{array}{c} \phi_{0,1}(x_{2i-1}^0, x_j^1) \\ \phi_{0,1}(x_{2i-1}^0 - 1, x_j^1) \end{array} \right)_{i=1, \dots, \frac{n}{2}, j=1, \dots, n} \prod_{r=1}^{M-1} \det(\phi_{r,r+1}(x_i^r, x_j^{r+1}))_{i,j=1}^n, \quad (5.1)$$

where n is assumed to be even and x_i^M ($i = 1, 2, \dots, n$) is fixed. As in the orthogonal case, this is slightly different from the weight of the multi-layer PNG model even if we take $n = N$, but we employ this for the moment and take the infinite particles limit when it becomes easy. The partition function and the probability of the non-intersecting paths are given by (3.2),(3.3) respectively. Again, our main focus is on the special case in (2.6),(2.7), but the results of this section do not depend on a specific choice of ϕ . For instance, when particles can hop only to nearest neighbor sites for each time, the determinantal process is a variant of the vicious walks with a condition that walkers start in pairs and end at neighboring sites [42].

Under this arrangement, we can show

Proposition 5.1.

$$\sum_{\bar{x}} \prod_{r=0}^{M-1} \prod_{j=1}^n (1 + g(r, x_j^r)) p_{n,M}(\bar{x}) = \sqrt{\det(1 + K_4 g)}, \quad (5.2)$$

where g is some function. The determinant on the right hand side is the Fredholm determinant, where K_4 is a 2×2 matrix kernel,

$$K_4(r_1, x_1; r_2, x_2) = \begin{bmatrix} S_4(r_1, x_1; r_2, x_2) & D_4(r_1, x_1; r_2, x_2) \\ I_4(r_1, x_1; r_2, x_2) & S_4(r_2, x_2; r_1, x_1) \end{bmatrix}, \quad (5.3)$$

with the matrix elements being

$$S_4(r_1, x_1; r_2, x_2) = \tilde{S}_4(r_1, x_1; r_2, x_2) - \phi_{r_1, r_2}(x_1, x_2), \quad (5.4)$$

$$\tilde{S}_4(r_1, x_1; r_2, x_2) = - \sum_{i,j=1}^n \phi_{r_1, M}(x_1, x_i^M) (A_4^{-1})_{i,j} G_4(r_2, x_2; M, x_j^M), \quad (5.5)$$

$$I_4(r_1, x_1; r_2, x_2) = \tilde{I}_4(r_1, x_1; r_2, x_2) - G_4(r_1, x_1; r_2, x_2), \quad (5.6)$$

$$\tilde{I}_4(r_1, x_1; r_2, x_2) = - \sum_{i,j=1}^n G_4(r_1, x_1; M, x_i^M) (A_4^{-1})_{i,j} G_4(r_2, x_2; M, x_j^M), \quad (5.7)$$

$$D_4(r_1, x_1; r_2, x_2) = \sum_{i,j=1}^n \phi_{r_1, M}(x_1, x_i^M) (A_4^{-1})_{i,j} \phi_{r_2, M}(x_2, x_j^M). \quad (5.8)$$

Here

$$(A_4)_{ij} = \sum_{y_1, y_2} s(y_2 - y_1) \phi_{0, M}(y_1, x_i^M) \phi_{0, M}(y_2, x_j^M), \quad (5.9)$$

$$G_4(r_1, x_1; r_2, x_2) = \sum_{y_1, y_2} s(y_2 - y_1) \phi_{0, r_1}(y_1, x_1) \phi_{0, r_2}(y_2, x_2), \quad (5.10)$$

$$s_{ij} = s(i - j) = \delta_{i+1, j} - \delta_{i, j+1}. \quad (5.11)$$

Remark. The subscript 4 refers to the fact that this case is related to the symplectic-unitary transition in random matrix theory. It should also be remarked that at this stage the infinite particles limit is taken easily. One only replaces the summation, $\sum_{i,j=1}^n$, in (5.5), (5.7), (5.8) with $\sum_{i,j=1}^\infty$.

Proof. As in the orthogonal case, we derive (5.2) by generalizing the methods of [19, 34]. Using the Heine identity (3.16), the partition function $Z_{n, M}[g]$ is written as

$$Z_{n, M}[g] = \frac{1}{(n!)^M} \sum_{x^0} \det \left(\begin{array}{c} \phi_{0, M}^g(x_{2i-1}^0, x_j^M) \\ \phi_{0, M}^g(x_{2i-1}^0 - 1, x_j^M) \end{array} \right)_{i=1, \dots, n/2, j=1, \dots, n}. \quad (5.12)$$

Here

$$\begin{aligned} \phi_{0, M}^g(x_i^0, x_j^M) &= \sum_{X_1, \dots, X_{M-1}} (1 + g(0, x_i^0)) \phi_{0, 1}(x_i^0, X_1) (1 + g(1, X_1)) \cdots \phi_{M-1, M}(X_{M-1}, x_j^M) \\ &= \phi_{0, M}(x_i^0, x_j^M) + (\phi_{0, r_1} \cdot g\psi_j)(x_i^0, x_j^M). \end{aligned} \quad (5.13)$$

In the second equality we have used ψ_j defined in (3.28). From (5.12), (5.13) and the identity [22, 35],

$$\begin{aligned} & \left(\sum_{x_1, \dots, x_n} \det(\phi_i(x_j) \psi_i(x_j))_{i=1 \dots 2n, j=1 \dots n} \right)^2 \\ &= ((2n)!)^2 \det \left(\sum_y (\phi_i(y) \psi_j(y) - \phi_j(y) \psi_i(y)) \right)_{i,j=1}^{2n}, \end{aligned} \quad (5.14)$$

one finds

$$Z_{n,M}[g]^2 = \det \left[(A_4)_{i,j} + (A_4^{(1)})_{i,j} + (A_4^{(2)})_{i,j} + (A_4^{(3)})_{i,j} \right]_{i,j=1}^n, \quad (5.15)$$

where A_4 is defined in (5.9) and

$$\begin{aligned} (A_4^{(1)})_{i,j} &= \sum_y [(\phi_{0,r_1} \cdot g\psi_j)(y, x_j^M) \phi_{0,M}(y+1, x_k^M) - \phi_{0,M}(y, x_k^M) (\phi_{0,r_1} \cdot g\psi_j)(y+1, x_j^M)] \\ &= \sum_{r,x} g\psi_i \cdot (G_4)_j \end{aligned} \quad (5.16)$$

$$\begin{aligned} (A_4^{(2)})_{i,j} &= \sum_y [\phi_{0,M}(y, x_j^M) (\phi_{0,r_1} \cdot g\psi_k)(y+1, x_k^M) - (\phi_{0,r_1} \cdot g\psi_k)(y, x_k^M) \phi_{0,M}(y+1, x_j^M)] \\ &= - \sum_{r,x} g\psi_j \cdot (G_4)_i \end{aligned} \quad (5.17)$$

$$\begin{aligned} (A_4^{(3)})_{i,j} &= \sum_y [(\phi_{0,r_1} \cdot g\psi_j)(y, x_j^M) (\phi_{0,r_1} \cdot g\psi_k)(y+1, x_k^M) \\ &\quad - (\phi_{0,r_1} \cdot g\psi_k)(y, x_k^M) (\phi_{0,r_1} \cdot g\psi_j)(y+1, x_j^M)] \\ &= - \sum_{r,x} g\psi_j \cdot G_4(g\psi_i). \end{aligned} \quad (5.18)$$

We should notice that the forms of $A_4^{(1)}$, $A_4^{(2)}$ and $A_4^{(3)}$ are the same as the corresponding ones in the orthogonal case, (3.29), (3.31) and (3.32), respectively. Only difference is that sgn in (3.12) and (3.13) is replaced by s , (5.11), in (5.9) and (5.10). Thus we can calculate the kernel along the line in section 3. The result is

$$\begin{aligned} &\left(\frac{Z_{n,M}[g]}{Z_{n,M}[0]} \right)^2 \\ &= \det \left(1 + \begin{bmatrix} -\sum_{i,j} \phi_i \otimes (A_4^{-1})_{i,j} (G_4)_j - \phi & \sum_{i,j} \phi_i \otimes (A_4^{-1})_{i,j} \phi_j \\ -\sum_{i,j} (G_4)_i \otimes (A_4^{-1})_{i,j} (G_4)_j - G_4 & \sum_{i,j} (G_4)_i \otimes (A_4^{-1})_{i,j} \phi_j - {}^t\phi \end{bmatrix} g \right). \end{aligned} \quad (5.19)$$

Recalling the definitions of ϕ_i and $(G_4)_i$, we see that (5.2) holds. \square

5.2 Scaling Limit

5.2.1 Generating Functions

The symbol $a_4(z)$ of the matrix A_4 is computed as

$$a_4(z) = f_{0,M} \left(\frac{1}{z} \right) s_4(z) f_{0,M}(z), \quad (5.20)$$

where

$$s_4(z) = \sum_{k \in \mathbb{Z}} s(k) z^k = -z + \frac{1}{z}. \quad (5.21)$$

The winding number of $a_4(z)$ is again not zero, but the difficulty can be overcome as in the orthogonal case. $s_4(z)$ can be expressed in two ways

$$s_4(z) = s_{4+}^{(1)}(z)s_{4-}^{(1)}(z) = s_{4+}^{(2)}(z)s_{4-}^{(2)}(z), \quad (5.22)$$

with

$$s_{4+}^{(1)}(z) = 1 + z, \quad s_{4-}^{(1)}(z) = -1 + \frac{1}{z}, \quad (5.23)$$

$$s_{4+}^{(2)}(z) = 1 - z, \quad s_{4-}^{(2)}(z) = 1 + \frac{1}{z}. \quad (5.24)$$

Then in terms of $a_{4+}^{(i)}, a_{4-}^{(i)}$ for $i = 1, 2$ defined by

$$a_{4+}^{(i)}(z) = f_{0,M;-} \left(\frac{1}{z} \right) f_{0,M;+}(z) s_{4+}^{(i)}(z), \quad (5.25)$$

$$a_{4-}^{(i)}(z) = f_{0,M;+} \left(\frac{1}{z} \right) f_{0,M;-}(z) s_{4-}^{(i)}(z), \quad (5.26)$$

A_4^{-1} is expressed as

$$A_4^{-1} = \frac{1}{2} \left\{ T \left(\frac{1}{a_{4+}^{(1)}} \right) T \left(\frac{1}{a_{4-}^{(1)}} \right) + T \left(\frac{1}{a_{4+}^{(2)}} \right) T \left(\frac{1}{a_{4-}^{(2)}} \right) \right\}. \quad (5.27)$$

Using the generating functions of A_4^{-1} and G_4 ,

$$\begin{aligned} & \sum_{i,j=1}^{\infty} z_1^{1-i} (A_4^{-1})_{i,j} z_2^{j-1} \\ &= \frac{z_1}{z_1 - z_2} \frac{1}{f_{0,M;-}(z_1) f_{0,M;+}(\frac{1}{z_1}) f_{0,M;+}(z_2) f_{0,M;-}(\frac{1}{z_2})} \frac{1}{2} \left\{ \frac{1}{s_{4+}^{(1)}(\frac{1}{z_1}) s_{4-}^{(1)}(\frac{1}{z_2})} + \frac{1}{s_{4+}^{(2)}(\frac{1}{z_1}) s_{4-}^{(2)}(\frac{1}{z_2})} \right\}, \\ (G_4)_{r_1, r_2}(z) &= -f_{0,r_1}(z) s_4(z) f_{0,r_2} \left(\frac{1}{z} \right), \end{aligned} \quad (5.28)$$

we can calculate the generating functions of $\tilde{S}_4, \tilde{I}_4, D_4$;

$$\begin{aligned}
\tilde{S}_4(r_1, z_1; r_2, z_2) &= \sum_{x_1, x_2 \in \mathbb{Z}} \tilde{S}_4(r_1, x_1; r_2, x_2) z_1^{x_1} z_2^{-x_2} \\
&= \frac{z_1}{z_1 - z_2} \frac{f_{r_1, M; -}(\frac{1}{z_1}) f_{0, r_2; +}(\frac{1}{z_2}) f_{0, M; -}(z_2)}{f_{0, M; -}(z_1) f_{0, r_1; +}(\frac{1}{z_1}) f_{r_2, M; -}(\frac{1}{z_2})} \frac{1}{2} \left\{ \frac{s_{4+}^{(1)}(\frac{1}{z_2})}{s_{4+}^{(1)}(\frac{1}{z_1})} + \frac{s_{4+}^{(2)}(\frac{1}{z_2})}{s_{4+}^{(2)}(\frac{1}{z_1})} \right\}, \\
&= \frac{(1 - \alpha)^{2(u_2 - u_1)} (1 - \alpha/z_1)^{N+u_1} (1 - \alpha z_2)^{N-u_2}}{(1 - \alpha z_1)^{N-u_1} (1 - \alpha/z_2)^{N+u_2}} \frac{z_1}{z_1 - z_2} \left\{ 1 + \frac{z_1 - z_2}{z_2(1 - z_1^2)} \right\}, \tag{5.29}
\end{aligned}$$

$$\begin{aligned}
\tilde{I}_4(r_1, z_1; r_2, z_2) &= \sum_{x_1, x_2 \in \mathbb{Z}} \tilde{I}_4(r_1, x_1; r_2, x_2) z_1^{x_1} z_2^{-x_2} \\
&= \frac{z_1}{z_1 - z_2} \frac{f_{0, r_1; +}(z_1) f_{0, M; -}(\frac{1}{z_1}) f_{0, r_2; +}(\frac{1}{z_2}) f_{0, M; -}(z_2)}{f_{r_1, M; -}(z_1) f_{r_2, M; -}(\frac{1}{z_2})} \\
&\quad \times \frac{1}{2} \left\{ s_{4-}^{(1)}\left(\frac{1}{z_1}\right) s_{4+}^{(1)}\left(\frac{1}{z_2}\right) + s_{4-}^{(2)}\left(\frac{1}{z_1}\right) s_{4+}^{(2)}\left(\frac{1}{z_2}\right) \right\}, \\
&= \frac{(1 - \alpha)^{2(u_1 + u_2)} (1 - \alpha/z_1)^{N-u_1} (1 - \alpha z_2)^{N-u_2}}{(1 - \alpha z_1)^{N+u_1} (1 - \alpha/z_2)^{N+u_2}} \frac{z_1}{z_1 - z_2} \left\{ -z_1 + \frac{1}{z_2} \right\}, \tag{5.30}
\end{aligned}$$

$$\begin{aligned}
\mathbb{D}_4(r_1, z_1; r_2, z_2) &= \sum_{x_1, x_2 \in \mathbb{Z}} D_4(r_1, x_1; r_2, x_2) z_1^{x_1} z_2^{-x_2} \\
&= \frac{z_1}{z_1 - z_2} \frac{f_{r_1, M; -}(\frac{1}{z_1}) f_{r_2, M; -}(z_2)}{f_{0, M; -}(z_1) f_{0, r_1; +}(\frac{1}{z_1}) f_{0, r_2; +}(z_2) f_{r_2, M; -}(\frac{1}{z_2})} \frac{1}{2} \left\{ \frac{1}{s_{4+}^{(1)}(\frac{1}{z_1}) s_{4-}^{(1)}(\frac{1}{z_2})} + \frac{1}{s_{4+}^{(2)}(\frac{1}{z_1}) s_{4-}^{(2)}(\frac{1}{z_2})} \right\} \\
&= \frac{(1 - \alpha/z_1)^{N+u_1} (1 - \alpha z_2)^{N+u_2}}{(1 - \alpha)^{2(u_1 + u_2)} (1 - \alpha z_1)^{N-u_1} (1 - \alpha/z_2)^{N-u_2}} \\
&\quad \times \frac{-z_1}{z_1 - z_2} \left\{ \frac{1}{2} \frac{1}{z_1 + 1} \frac{1}{1 - z_2} + \frac{1}{2} \frac{1}{1 - z_1} \frac{1}{1 + z_2} \right\}. \tag{5.31}
\end{aligned}$$

5.2.2 Bulk

In the bulk region, the asymptotic behavior is just the same as in the orthogonal case.

Proposition 5.2. *For the scaled height variable defined by (4.26), (4.30) holds in the symplectic case as well.*

Proof. To show this, we need the asymptotics of \tilde{S}_4, \tilde{I}_4 and D_4 in the bulk region. Applying the same reasoning as in 4.2, one finds

$$\begin{aligned}
\tilde{S}_4 &\sim (1 - \alpha)^{2(u_2 - u_1)} (p_c(\beta_0))^{(\xi_2 - \xi_1)d(\beta_0)N^{1/3}} \frac{1}{d(\beta_0)N^{1/3}} \\
&\quad e^{G_1(\beta_0)c(\beta_0)N^{2/3}(\tau_1 - \tau_2) + G_2(\beta_0)c(\beta_0)^2N^{1/3}(\tau_1^2 - \tau_2^2) + G_3(\beta_0)c(\beta_0)^3(\tau_1^3 - \tau_2^3) + \xi_2\tau_2 - \xi_1\tau_1} \\
&\quad \frac{1}{4\pi^2} \int_{\text{Im}w_1 = \eta_1} dw_1 \int_{\text{Im}w_2 = \eta_2} dw_2 \left(-\frac{1}{\tau_2 - \tau_1 + i(w_1 + w_2)} \right) e^{i\xi_1 w_1 + i\xi_2 w_2 + \frac{i}{3}(w_1^3 + w_2^3)}. \tag{5.32}
\end{aligned}$$

$$\begin{aligned} \tilde{I}_4 &\sim (1-\alpha)^{2(u_1+u_2)} \frac{p_c(-\beta_0)^3}{(1-p_c(-\beta_0)^2)} (p_c(\beta_0))^{(\xi_1+\xi_2)d(\beta_0)N^{1/3}} \frac{1}{d(\beta_0)^3 N} \\ &\quad e^{-2N\lambda_0(\beta_0)-\lambda_1(\beta_0)c(\beta_0)N^{2/3}(\tau_1+\tau_2)-\lambda_2(\beta_0)c(\beta_0)^2N^{1/3}(\tau_1^2+\tau_2^2)-\lambda_3(\beta_0)c(\beta_0)^3(\tau_1^3+\tau_2^3)+\xi_1\tau_1+\xi_2\tau_2} \\ &\quad \frac{-1}{4\pi^2} \int_{\text{Im}w_1=\eta_1} dw_1 \int_{\text{Im}w_2=\eta_2} dw_2 (\tau_1 - \tau_2 + i(w_1 - w_2)) e^{i\xi_1 w_1 + i\xi_2 w_2 + \frac{i}{3}(w_1^3 + w_2^3)}, \end{aligned} \quad (5.33)$$

$$\begin{aligned} D_4 &\sim (1-\alpha)^{-2(u_1+u_2)} \frac{p_c(\beta_0)^4}{(1-p_c(\beta_0)^2)^3} (p_c(\beta_0))^{-(\xi_1+\xi_2)d(\beta_0)N^{1/3}} \frac{1}{d(\beta_0)^3 N} \\ &\quad e^{2N\lambda_0(\beta_0)+\lambda_1(\beta_0)c(\beta_0)N^{2/3}(\tau_1+\tau_2)+\lambda_2(\beta_0)c(\beta_0)^2N^{1/3}(\tau_1^2+\tau_2^2)+\lambda_3(\beta_0)c(\beta_0)^3(\tau_1^3+\tau_2^3)-\xi_1\tau_1-\xi_2\tau_2} \\ &\quad \frac{1}{4\pi^2} \int_{\text{Im}w_1=\eta_1} dw_1 \int_{\text{Im}w_2=\eta_2} dw_2 (\tau_1 - \tau_2 - i(w_1 - w_2)) e^{i\xi_1 w_1 + i\xi_2 w_2 + \frac{i}{3}(w_1^3 + w_2^3)}. \end{aligned} \quad (5.34)$$

Then discussions similar to ones below (4.81) lead to (4.30). \square

5.2.3 Near the origin

Next we show that the fluctuation near the origin is described by the process which gives the symplectic-unitary transition in random matrix theory [28]. Namely, if we define the scaled height variable as (4.83), one can show

Theorem 5.3.

$$\lim_{N \rightarrow \infty} \mathbb{P}[H_N(\tau_1) \leq s_1, \dots, H_N(\tau_m) \leq s_m] = \sqrt{\det(1 + \mathcal{K}_4 \mathcal{G})}, \quad (5.35)$$

where $\mathcal{G}(\tau_j, \xi) = -\chi_{(s_j, \infty)}(\xi)$ ($j = 1, 2, \dots, m$) and \mathcal{K}_4 is the 2×2 matrix kernel, for which a representative element is given by

$$\mathcal{K}_4(\tau_1, \xi_1; \tau_2, \xi_2) = \begin{bmatrix} \mathcal{S}_4(\tau_1, \xi_1; \tau_2, \xi_2) & \mathcal{D}_4(\tau_1, \xi_1; \tau_2, \xi_2) \\ \mathcal{I}_4(\tau_1, \xi_1; \tau_2, \xi_2) & \mathcal{S}_4(\tau_2, \xi_2; \tau_1, \xi_1) \end{bmatrix}, \quad (5.36)$$

with the matrix elements being

$$\mathcal{S}_4(\tau_1, \xi_1; \tau_2, \xi_2) = \tilde{\mathcal{S}}_4(\tau_1, \xi_1; \tau_2, \xi_2) - \Phi_{\tau_1, \tau_2}(\xi_1, \xi_2), \quad (5.37)$$

$$\tilde{\mathcal{S}}_4(\tau_1, \xi_1; \tau_2, \xi_2) = \int_0^\infty d\lambda e^{-\lambda(\tau_1 - \tau_2)} \text{Ai}(\xi_1 + \lambda) \text{Ai}(\xi_2 + \lambda) - \frac{1}{2} \text{Ai}(\xi_2) \int_{\xi_1}^\infty d\lambda e^{-\lambda\tau_1} \text{Ai}(\xi_2 - \lambda), \quad (5.38)$$

$$\begin{aligned} \mathcal{I}_4(\tau_1, \xi_1; \tau_2, \xi_2) &= - \int_0^\infty d\lambda e^{-\lambda\tau_1} \text{Ai}(\xi_1 - \lambda) \frac{d}{d\lambda} \{ e^{-\lambda\tau_2} \text{Ai}(\xi_2 - \lambda) \} \\ &\quad + \int_0^\infty d\lambda e^{-\lambda\tau_2} \text{Ai}(\xi_2 - \lambda) \frac{d}{d\lambda} \{ e^{-\lambda\tau_1} \text{Ai}(\xi_1 - \lambda) \} \end{aligned} \quad (5.39)$$

$$\begin{aligned} \mathcal{D}_4(\tau_1, \xi_1; \tau_2, \xi_2) &= \frac{1}{4} \int_0^\infty d\lambda e^{-\lambda\tau_1} \text{Ai}(\xi_1 + \lambda) \int_\lambda^\infty dv e^{-v\tau_2} \text{Ai}(\xi_2 + v) \\ &\quad - \frac{1}{4} \int_0^\infty d\lambda e^{-\lambda\tau_2} \text{Ai}(\xi_2 + \lambda) \int_\lambda^\infty dv \text{Ai}(\xi_1 + v). \end{aligned} \quad (5.40)$$

Definition of $\Phi_{\tau_1, \tau_2}(\xi_1, \xi_2)$ is already given in (4.34).

Remark. For $\tau = 0$, we have

$$\lim_{N \rightarrow \infty} \mathbb{P}[H_N(0) \leq s] = F_4(s), \quad (5.41)$$

where $F_4(s)$ is the GSE Tracy-Widom distribution [22]. Notice a notational difference in [22] and [25]. We follow the convention in the latter; our $F_4(s)$ is $F_4(s) = F_4^{\text{BR}}(s) = F_4^{\text{TW}}(\sqrt{2}s)$. The result, (5.41), was shown in [25]; it would also be possible to prove this by using

$$\mathbb{P}[h(0, 2N) \leq X] = \frac{1}{Z_N^{(4)}} \sum_{\substack{h \in \mathbb{N}^{\frac{N}{2}} \\ \max\{h_j\} \leq X+N-1}} \prod_{1 \leq i < j \leq \frac{N}{2}} (h_i - h_j)^2 (h_i - h_j + 1)(h_i - h_j - 1) \prod_{i=1}^{\frac{N}{2}} q^{h_i}, \quad (5.42)$$

and the skew orthogonal polynomials techniques [43, 44, 45]. The Meixner symplectic ensemble representation, (5.42), was not given in [6] but can be proved similarly if one notices that a symmetric $N \times N$ matrix with zero elements on diagonal and non-negative integer elements on off-diagonal is mapped to a semistandard Young tableau with all columns of even length through Knuth correspondence [46].

Proof. Derivation of (5.35) is analogous to that of (4.87). Using the integral representation of the Airy function, (4.97), we have, for $\tilde{\mathcal{S}}_4$,

$$\begin{aligned} & \tilde{\mathcal{S}}_4(\tau_1, \xi_1; \tau_2, \xi_2) \\ &= \frac{1}{4\pi^2} \int_{\text{Im}w_1=\eta_1} dw_1 \int_{\text{Im}w_2=\eta_2} dw_2 \left(-\frac{1}{\tau_2 - \tau_1 + i(w_1 + w_2)} - \frac{1}{2(\tau_1 - iw_1)} \right) \\ & \quad e^{i\xi_1 w_1 + i\xi_2 w_2 + \frac{i}{3}(w_1^3 + w_2^3)}, \end{aligned} \quad (5.43)$$

where $\eta_1 + \eta_2 + \tau_1 - \tau_2 > 0$. For \mathcal{I}_4 ,

$$\begin{aligned} & \mathcal{I}_4(\tau_1, \xi_1; \tau_2, \xi_2) \\ &= \frac{-1}{4\pi^2} \int_{\text{Im}w_1=\eta_1} dw_1 \int_{\text{Im}w_2=\eta_2} dw_2 \frac{\tau_2 + iw_2}{(\tau_1 + \tau_2 + i(w_1 + w_2))} e^{i\xi_1 w_1 + i\xi_2 w_2 + \frac{i}{3}(w_1^3 + w_2^3)} \\ & \quad - (\tau_1, \xi_1 \leftrightarrow \tau_2, \xi_2), \end{aligned} \quad (5.44)$$

where $\tau_1 + \tau_2 - \eta_1 - \eta_2 > 0$. For \mathcal{D}_4 ,

$$\begin{aligned} & \mathcal{D}_4(\tau_1, \xi_1; \tau_2, \xi_2) \\ &= \frac{1}{4\pi^2} \int_{\text{Im}w_1=\eta_1} dw_1 \int_{\text{Im}w_2=\eta_2} dw_2 \frac{1}{4(\tau_1 - iw_1)(\tau_1 + \tau_2 - i(w_1 + w_2))} e^{i\xi_1 w_1 + i\xi_2 w_2 + \frac{i}{3}(w_1^3 + w_2^3)} \\ & \quad - (\tau_1, \xi_1 \leftrightarrow \tau_2, \xi_2), \end{aligned} \quad (5.45)$$

where there is no additional condition on $\tau_1, \tau_2, \eta_1, \eta_1$. Then applying the same method as in 4.3, we can show

$$S_4(r_1, x_1; r_2, x_2) \sim e^{(\tau_2^3 - \tau_1^3)/3 + \xi_1 \tau_1 - \xi_2 \tau_2} dN^{1/3} \mathcal{S}_4(\tau_1, \xi_1; \tau_2, \xi_2), \quad (5.46)$$

$$I_4(r_1, x_1; r_2, x_2) \sim e^{(\tau_1^3 + \tau_2^3)/3 - \xi_1 \tau_1 - \xi_2 \tau_2} d^2 N^{2/3} \mathcal{L}_4(\tau_1, \xi_1; \tau_2, \xi_2), \quad (5.47)$$

$$D_4(r_1, x_1; r_2, x_2) \sim e^{-(\tau_1^3 + \tau_2^3)/3 + \xi_1 \tau_1 + \xi_2 \tau_2} \mathcal{D}_4(\tau_1, \xi_1; \tau_2, \xi_2), \quad (5.48)$$

from which (5.35) follows. \square

6 Continuous Limit

Let us take the limit $\alpha \rightarrow 0, N \rightarrow \infty$ with $t = \alpha N$, fixed. In this limit time and space become continuous; the time variable t can take any positive value whereas the scaled space variable is defined to be $v = \alpha r/2$. The model is reduced to the standard PNG model in a half space ($v \geq 0$) with an external source at the origin. As in the discrete case, we extend the space to the whole space ($v \in \mathbb{R}$), putting the symmetry condition on the height with respect to the origin. First we have a flat substrate. At time 0, a nucleation of a height one occurs at the origin. This step grows laterally in both directions with unit speed. Above this ground layer there occur other nucleations with rate two per unit length. The height of a nucleation is always one. There is an external source at the origin with rate γ . As in the discrete case, one can define the multi-layer version [14].

It is easy to take this limit at the level of the generating functions. For the orthogonal case, (4.22),(4.23),(4.24) become

$$\tilde{\mathbb{S}}_1 \sim e^{2(v_1 - v_2)} e^{t(z_1 - 1/z_1) - v_1(z_1 + 1/z_1)} e^{t(1/z_2 - z_2) + v_2(z_2 + 1/z_2)} \frac{z_1}{z_1 - z_2} \left\{ 1 + \frac{z_1 - z_2}{(1 + z_1)(z_2 - 1)} \right\}, \quad (6.1)$$

$$\tilde{\mathbb{I}}_1 \sim e^{-2(v_1 + v_2)} e^{t(z_1 - 1/z_1) + v_1(z_1 + 1/z_1)} e^{t(1/z_2 - z_2) + v_2(z_2 + 1/z_2)} \frac{z_1}{z_1 - z_2} \left\{ \frac{1}{2} \frac{z_2 + 1}{z_2 - 1} - \frac{1}{2} \frac{1 + z_1}{1 - z_1} \right\}, \quad (6.2)$$

$$\tilde{\mathbb{D}}_1 \sim e^{2(v_1 + v_2)} e^{t(z_1 - 1/z_1) + v_1(z_1 + 1/z_1)} e^{t(1/z_2 - z_2) + v_2(z_2 + 1/z_2)} \frac{z_1}{z_1 - z_2} \left\{ \frac{1}{2} \frac{z_1 - 1}{z_1 + 1} - \frac{1}{2} \frac{1 - z_2}{1 + z_2} \right\}. \quad (6.3)$$

Expressions for the symplectic case are given by (6.1),(6.2),(6.3) with the last factors replaced by the corresponding ones in (5.29),(5.30),(5.31).

The scaling limit can also be studied as in the discrete PNG model. First the thermodynamic shape is known to be

$$h(v = \beta_0 t, t)/t \sim 2\sqrt{1 - \beta_0^2}, \quad (6.4)$$

where $0 < \beta_0 < 1$ is fixed [1]. To consider the scaling limit in the bulk, define the scaled height variable as

$$H_N(\tau, \beta_0) = \frac{h(v = \beta_0 t + c(\beta_0)t^{\frac{2}{3}}\tau, t) - a(\beta_0 + \frac{c(\beta_0)\tau}{t^{1/3}})t}{d(\beta_0)t^{\frac{1}{3}}}, \quad (6.5)$$

where

$$a(\beta) = 2\sqrt{1 - \beta^2}, \quad (6.6)$$

$$d(\beta) = (1 - \beta^2)^{\frac{1}{6}}, \quad (6.7)$$

$$c(\beta) = (1 - \beta^2)^{\frac{7}{6}}. \quad (6.8)$$

Then one can show

Proposition 6.1. *For the scaled height variable defined by (6.5), (4.30) holds.*

The proof of the Proposition 6.1 is parallel to that in 4.2. The main difference is that the function $g_{\mu,\beta}$ in (4.42) is replaced by a simpler

$$g_{\mu,\beta}(z) = z - \frac{1}{z} - \beta(z + \frac{1}{z}) - \mu \log z, \quad (6.9)$$

for which the double critical point is

$$\mu_c(\beta) = 2\sqrt{1 - \beta^2}, \quad (6.10)$$

$$p_c(\beta) = \sqrt{\frac{1 + \beta}{1 - \beta}}. \quad (6.11)$$

As for the fluctuation near the origin, if we define the scaled height variable as

$$H_N(\tau) = \frac{h(v = t^{\frac{2}{3}}\tau, t) - 2t}{t^{\frac{1}{3}}} + \tau^2, \quad (6.12)$$

we have

Proposition 6.2. *For the scaled height variable defined by (6.12), one has (4.87) for the orthogonal case and (5.35) for the symplectic case.*

7 Discussions

In the preceding sections, we have given a detailed analysis of the height fluctuation of the model for two special values of the strength of the external source at the origin, $\gamma = 1$ and $\gamma = 0$. Our results show that the fluctuation near the origin is described by the orthogonal/symplectic to unitary transition in random matrix theory.

This implies, in particular, that the height fluctuation of the PNG model at a single point near the origin is equivalent to that of the largest eigenvalue of the transition ensemble. To check this, we performed Monte-Carlo simulations of the PNG model and the transition random matrix. In Figs. 4 and 5, we have shown the fluctuations of the height of the PNG model and the largest eigenvalue of the transition ensemble. We see an excellent agreement between them.

Unfortunately properties of the transition ensemble have not been well studied compared to the ensembles with a specified symmetry. For example, it seems difficult to numerically compute the probability distribution function of the largest eigenvalue. This is sharply contrasted to the situation for the GUE/GOE/GSE, for which the Painlevé representation allows us to plot the probability distribution function with high accuracy. It would be desirable to study the transition ensemble to better understand the statistical properties of the PNG model.

Now we argue what happens for other values of γ . For the fluctuation at the origin, the results have been obtained in [25] where a strong universality is observed. The GSE Tracy-Widom distribution describes the fluctuation not only for $\gamma = 0$ but also for all values in $0 \leq \gamma < 1$. The fluctuation becomes the Gaussian for all values in $\gamma > 1$. On the other hand, the GOE Tracy-Widom distribution appears only at $\gamma = 1$. The Gaussian fluctuation for $\gamma > 1$ is stated only for the continuous model in [25], but is expected to persist for the discrete model as well. In Fig. 6, typical shapes of the droplet are shown for three cases where $\gamma < 1$, $\gamma = 1$, $\gamma > 1$. From these one should be able to guess that the shape looks similar for all values in $\gamma \leq 1$ but a cusp-like piece appears near the origin when γ becomes greater than unity.

This suggests that the fluctuation near the origin also has a similar universality. For all values in $0 \leq \gamma < 1$, it is expected to be described by the symplectic-unitary transition. This is a conjecture because we do not know how to prove this at present, but is supported by a Monte-Carlo simulation. See Fig. 7, where a good agreement is observed.

For $\gamma > 1$, we can also expect some universal behavior for the fluctuation near the origin. We have not found a compact formula for general γ , but the situation becomes quite simple in the limiting case where $\alpha \rightarrow 0$ with $0 < \gamma\alpha < 1$ fixed. In this limit, the nucleations in the bulk are so rare that the only those at the origin are important. Then the height at a position r and at time t would be almost the same as that at a position 0 and at time $t - r$. Therefore the height fluctuation at a single point is given by the Gaussian. If we set $r = \rho t$ with $0 < \rho < 1$ fixed, we have

$$\lim_{t \rightarrow \infty} \mathbb{P} \left(\frac{h(r, t) - (1 - \rho)a_G t}{(1 - \rho)^{\frac{1}{2}} d_G t^{\frac{1}{2}}} \leq s \right) = \frac{1}{\sqrt{2\pi}} \int_{-\infty}^s e^{-\frac{\xi^2}{2}} d\xi = \text{erf}(s) \quad (7.1)$$

where $a_G = \frac{\gamma\alpha}{1-\gamma\alpha}$ and $d_G = \frac{1}{1-\gamma\alpha}$. A result of a Monte-Carlo simulation corresponding to this case is shown in Fig. 8. In addition, since nucleations at the origin are independent for each time, the multi-point equal time height fluctuation would be described by the one-dimensional Brownian motion. The situation would be somewhat more difficult for a smaller γ , but we expect that the same Gaussian fluctuation is observed in an appropriate

limit.

8 Conclusion

In this paper, we have studied fluctuation properties of the one-dimensional polynuclear growth (PNG) model in a half space with an external source at the origin. We have mainly considered the model in a discrete space and time, but have also given results for the model in a continuous setting. The results in the scaling limit are the same for both cases.

For two special values of the strength of the external source, γ , we have performed a detailed analysis. The $\gamma = 1$ case corresponds to a critical point, which we call the orthogonal case. The $\gamma = 0$ case corresponds to the model without the external source, which we call the symplectic case. The main results are (4.87) for the orthogonal case, and (5.35) for the symplectic case. According to these the height fluctuation of the model near the origin is equivalent to those of the largest eigenvalue of the orthogonal/symplectic to unitary transition ensemble at soft edge in random matrix theory. We have also shown that the height fluctuation at bulk is described by the Airy process. For other values of γ , we have conjectured that the fluctuation is the symplectic-unitary type for $0 \leq \gamma < 1$, whereas it is the Gaussian type for $\gamma > 1$. Some Monte-Carlo simulation results are also presented to confirm our results and conjectures.

Acknowledgment

The authors would like to thank H. Spohn, M. Katori, T. Nagao, M. Prähofer and P. Ferrari for useful discussions and comments. The first author is grateful to the Zentrum Mathematik, TU München and in particular to H. Spohn for kind hospitality during his stay. He also thanks T. Miyake and Y. Saiga for advice on numerical diagonalization of matrices.

References

- [1] J. Krug and H. Spohn. Kinetic roughening of growing interfaces. In C. Godrèche, editor, *Solids far from Equilibrium: Growth, Morphology and Defects*, pages 479–582, 1992.
- [2] P. Meakin. *Fractals, scaling and growth far from equilibrium*. Cambridge, 1998.
- [3] M. Kardar, G. Parisi and Y. C. Zhang. Dynamic scaling of growing interfaces. *Phys. Rev. Lett.*, 56:889–892, 1986.
- [4] L.-H. Gwa and H. Spohn. Six-vertex model, roughened surfaces, and an asymmetric spin Hamiltonian. *Phys. Rev. Lett.*, 68:725–728, 1992.

- [5] D. Kim. Bethe ansatz solution for crossover scaling functions of the asymmetric XXZ chain and the Kardar-Parisi-Zhang-type growth model. *Phys. Rev. E*, 52:3512–3524, 1995.
- [6] K. Johansson. Shape fluctuations and random matrices. *Commun. Math. Phys.*, 209:437–476, 2000.
- [7] M. Prähofer and H. Spohn. Universal distributions for growth processes in 1+1 dimensions and random matrices. *Phys. Rev. Lett*, 84:4882–4885, 2000.
- [8] M. Prähofer and H. Spohn. Statistical self-similarity of one-dimensional growth processes. *Physica A*, 279:342–352, 2000.
- [9] J. Baik and E. M. Rains. Limiting distributions for a polynuclear growth model with external sources. *J. Stat. Phys.*, 100:523–541, 2000.
- [10] J. Gravner, C. A. Tracy and H. Widom. Limit theorems for height fluctuations in a class of discrete space and time growth models. *J. Stat. Phys.*, 102:1085–1132, 2001.
- [11] J. Gravner, C. A. Tracy and H. Widom. A growth model in a random environment. *Ann. Probab.*, 30:1340–1369, 2002.
- [12] J. Gravner, C. A. Tracy and H. Widom. Fluctuations in the composite regime of a disordered growth model. *Commun. Math. Phys.*, 229:433–458, 2002.
- [13] M. Prähofer and H. Spohn. Current fluctuations for the totally asymmetric simple exclusion process. In V. Sidoravicius, editor, *In and out of equilibrium, vol. 51 of Progress in Probability*, pages 185–204, 2002.
- [14] M. Prähofer and H. Spohn. Scale invariance of the PNG droplet and the Airy process. *J. Stat. Phys.*, 108:1071–1106, 2002.
- [15] M. Prähofer and H. Spohn. Exact scaling functions for one-dimensional stationary KPZ growth. cond-mat/0212519.
- [16] J. Baik, P. A. Deift and K. Johansson. On the distribution of the length of the longest increasing subsequence in a random permutation. *J. Amer. Math. Soc.*, 12:1119–1178, 1999.
- [17] D. Aldous and P. Diaconis. Longest increasing subsequences: from patience sorting to the Baik-Deift-Johansson theorem. *Bull. Amer. Math. Soc.*, 36:413–432, 1999.
- [18] K. Johansson. Non-intersecting paths, random tilings and random matrices. *Probab. Theory Relat. Fields*, 123:225–280, 2002.
- [19] K. Johansson. Discrete polynuclear growth and determinantal processes. math.PR/0206208.

- [20] C. A. Tracy and H. Widom. Level-spacing distributions and the Airy kernel. *Commun. Math. Phys.*, 159:151–174, 1994.
- [21] M. L. Mehta. *Random Matrices*. Academic, 2nd edition, 1991.
- [22] C. A. Tracy and H. Widom. On orthogonal and symplectic matrix ensembles. *Commun. Math. Phys.*, 177:727–754, 1996.
- [23] J. Baik and E. M. Rains. Algebraic aspects of increasing subsequences. *Duke Math. J.*, 109:1–65, 2001.
- [24] J. Baik and E. M. Rains. The asymptotics of monotone subsequences of involutions. *Duke Math. J.*, 109:205–281, 2001.
- [25] J. Baik and E. M. Rains. Symmetrized random permutations. In P. M. Bleher and A. R. Its, editors, *Random Matrix Models and Their Applications*, pages 1–29, 2001.
- [26] F. J. Dyson. A Brownian-motion model for the eigenvalues of a random matrix. *J. Math. Phys.*, 3:1191–1198, 1962.
- [27] K. Johansson. Discrete orthogonal polynomial ensembles and the Plancherel measure. *Annals of Math.*, 153:259–296, 2001.
- [28] P. J. Forrester, T. Nagao and G. Honner. Correlations for the orthogonal-unitary and symplectic transitions at the hard and soft edges. *Nucl. Phys. B*, 553:601–643, 1999.
- [29] S. Karlin and L. McGregor. Coincidence properties of birth and death processes. *Pacific J.*, 9:1109–1140, 1959.
- [30] S. Karlin and L. McGregor. Coincidence probabilities. *Pacific J.*, 9:1141–1164, 1959.
- [31] J. Baik. Random vicious walks and random matrices. *Comm. Pure Appl. Math.*, 53:1385–1410, 2000.
- [32] T. Nagao and P. J. Forrester. Vicious random walkers and a discretization of Gaussian random matrix ensembles. *Nucl. Phys. B*, 620:551–565, 2002.
- [33] T. Nagao, M. Katori and H. Tanemura. Dynamical correlations among vicious random walkers. *Phys. Lett. A*, 307:29–35, 2003.
- [34] C. A. Tracy and H. Widom. Correlation functions, cluster functions, and spacing distributions for random matrices. *J. Stat. Phys.*, 92:809–835, 1998.
- [35] N. G. de Bruijn. On some multiple integrals involving determinants. *J. Indian Math. Soc.*, 19:133–151, 1955.
- [36] See for instance Ch. 9 of B. M. McCoy and T. T. Wu. *The Two-Dimensional Ising Model*. Harvard University Press, 1973.

- [37] H. Rost. Non-equilibrium behavior of a many particle process: Density profile and local equilibria. *Zeitschrift f. Warsch. Verw. Gebiete*, 58:41–53, 1981.
- [38] A. M. S. Macêdo. Universal parametric correlations at the soft edge of spectrum of random matrix ensembles. *Europhys. Lett.*, 26:641–646, 1994.
- [39] T. Nagao and P. J. Forrester. Multilevel dynamical correlation functions for Dyson’s Brownian motion model of random matrices. *Phys. Lett. A*, 247:42–46, 1998.
- [40] C. A. Tracy and H. Widom. System of differential equations for the Airy process. math.PR/0302033.
- [41] M. Adler and P. van Moerbeke. A PDE for the joint distributions of the Airy process. math.PR/0302329.
- [42] M. Katori and H. Tanemura, in preparation.
- [43] T. Nagao and M. Wadati. Correlation functions of random matrix ensembles related to classical orthogonal polynomials. *J. Phys. Soc. Jpn*, 60:3298–3322, 1991.
- [44] T. Nagao and M. Wadati. Correlation functions of random matrix ensembles related to classical orthogonal polynomials ii. *J. Phys. Soc. Jpn*, 61:78–88, 1992.
- [45] T. Nagao and M. Wadati. Correlation functions of random matrix ensembles related to classical orthogonal polynomials iii. *J. Phys. Soc. Jpn*, 61:1910–1918, 1992.
- [46] W. H. Burge. Four correspondences between graphs and generalized Young tableaux. *J. Comb. Th. (A)*, 17:12–30, 1974.

Figure Captions

Fig. 1: Dynamical rules of the discrete PNG model. (a) At time t , a nucleation of a height k occurs at site r with probability $(1 - q)q^k$ when $r \neq 0$ and $(1 - \gamma\sqrt{q})(\gamma\sqrt{q})^k$ when $r = 0$. Once the nucleation occurs, it grows laterally toward right and left with unit speed. (b) When two steps collide, the one with higher height swallow the one with lower height. In the multi-layer version, a nucleation occurs in the lower layer at the position above which the collision occurs in the upper layer. The height is equal to the height of the swallowed region in the upper layer.

Fig. 2: An example of the multi-layer PNG heights for the $\gamma = 1$ case for $q = 0.25$ at (a) $t = 6$ (b) $t = 100$. It looks symmetric with respect to $r = 1/2$. The limiting shape is also shown as a dotted line for (b).

Fig. 3: An example of the multi-layer PNG heights for the $\gamma = 0$ case for $q = 0.25$ at $t = 100$. Each neighboring two heights form a pair at $r = 0$. The limiting shape is also shown as a dotted line.

Fig. 4: Probability distributions of the scaled height of the PNG model for $\gamma = 1$ and the scaled largest eigenvalue of the orthogonal-unitary transition random matrix ensemble. For the PNG model, the parameters are for $q = 0.25$, $t = 2000$, and (a) $r = 0$ (b) $r = 330$ (c) $r = 1000$ (each 10000 samples). The first two cases correspond to (a) $\tau = 0$ (b) $\tau = 1$, in which the scaling (4.83) is used. The case (c) is better fitted to the bulk scaling limit; the scaling (4.26) is used. In the figures, they are represented as circles. For the transition random matrix ensemble, the data are for $N = 500$, (a) $\tau = 0$ (b) $\tau = 1$ (c) $\tau = 10$ (each 1000 samples). In the figures, they are represented as +. For (a)(resp. (c)), the GOE (resp. GUE) Tracy-Widom distribution is also shown as a solid line.

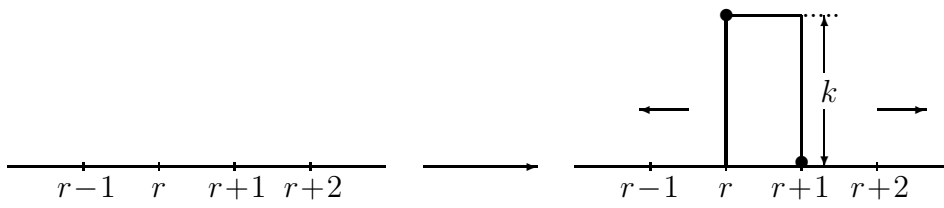
Fig. 5: Probability distributions of the scaled height of the PNG model for $\gamma = 0$ and the scaled largest eigenvalue of the symplectic-unitary transition random matrix ensemble. For the PNG model, the parameters are for $q = 0.25$, $t = 2000$, and (a) $r = 0$ (b) $r = 330$ (c) $r = 1000$ (each 10000 samples). The first two cases correspond to (a) $\tau = 0$ (b) $\tau = 1$, in which the scaling (4.83) is used. The case (c) is better fitted to the bulk scaling limit; the scaling (4.26) is used. In the figures, they are represented as circles. For the transition random matrix ensemble, the data are for $N = 200$, (a) $\tau = 0$ (b) $\tau = 1$ (c) $\tau = 10$ (each 10000 samples). In the figures, they are represented as +. For (a)(resp. (c)), the GSE (resp. GUE) Tracy-Widom distribution is also shown as a solid line.

Fig. 6: Typical droplet shapes for three values of $\gamma = 0.8, 1.0$ and 1.2 , which are fairly close to the critical value $\gamma = 1$. The model parameters are taken to be $t = 1000, q = 0.25$. Notice that the appearance of the shape changes drastically when γ gets greater than one.

Fig. 7: Probability distributions of the scaled height of the PNG model for $\gamma = 0.5$ and the scaled largest eigenvalue of the symplectic-unitary transition random matrix ensemble. Parameters are the same as those for Fig. 5.

Fig. 8: Probability distributions of the scaled height of the PNG model for $q = 0.0001, \gamma = 50$ and the Gaussian distribution (solid line). For the PNG model, the parameters are $t = 2000$ and $r = 0$ (+), $r = 330$ (\circ), $r = 1000$ (\bullet) (each 10000 samples).

(a)



(b)

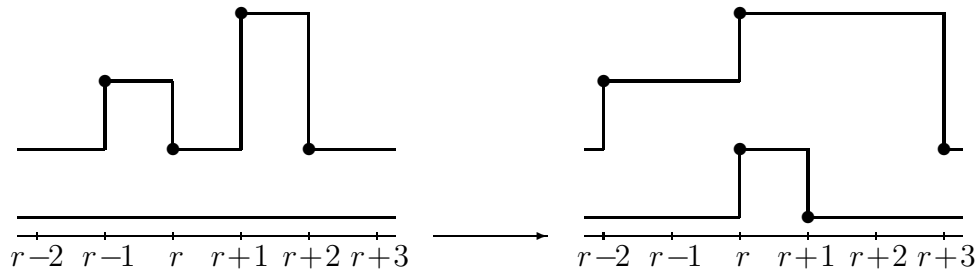
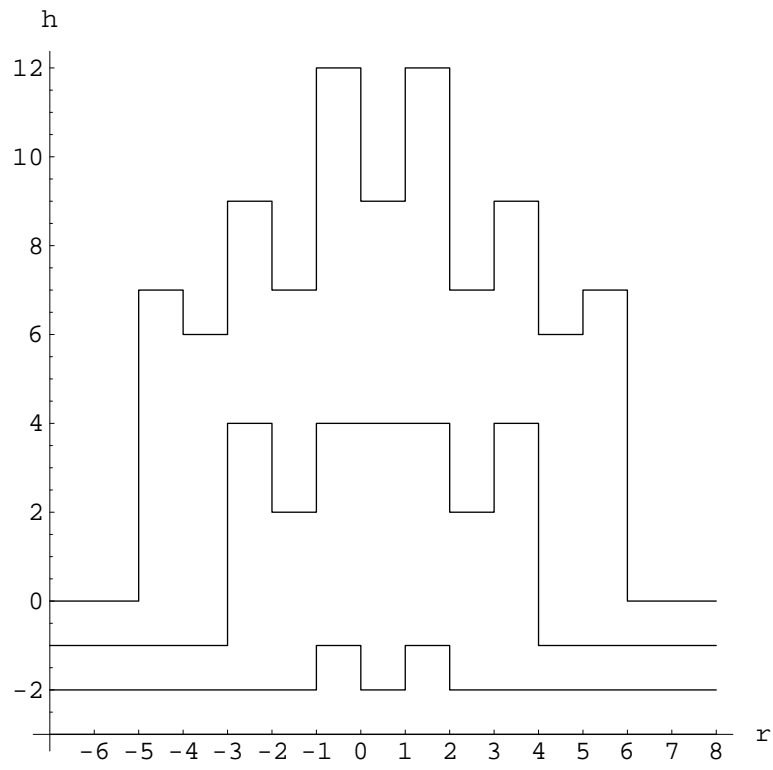


Figure 1

(a)



(b)

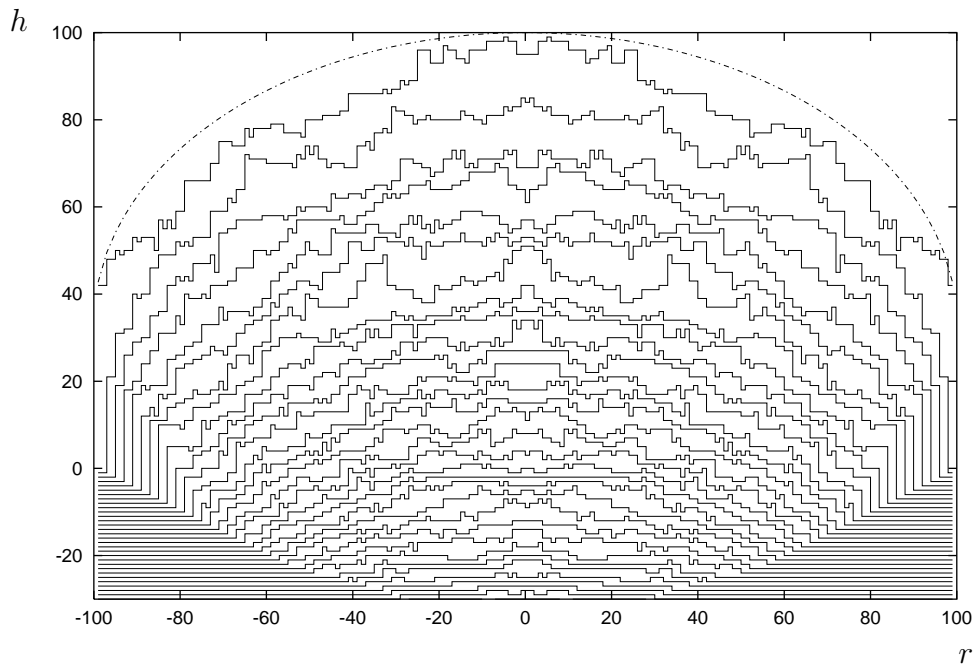


Figure 2

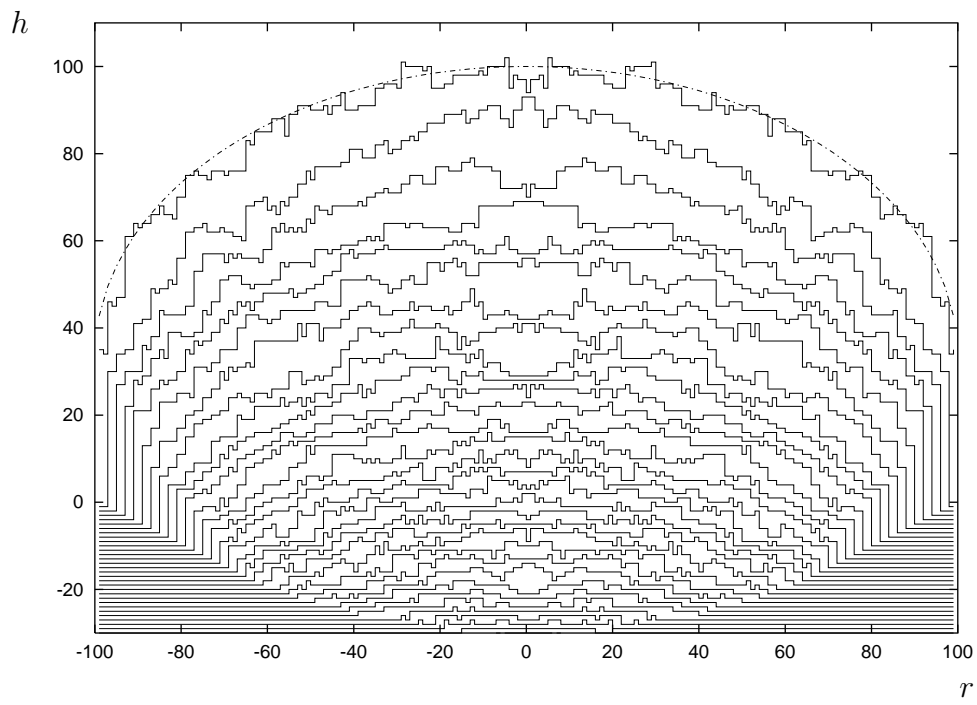


Figure 3

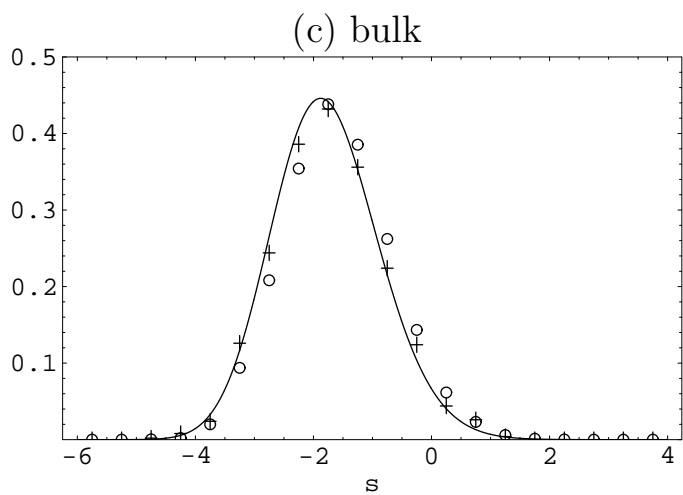
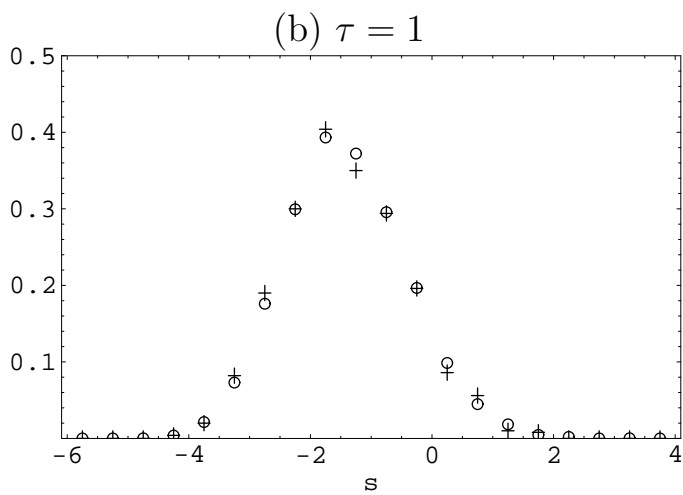
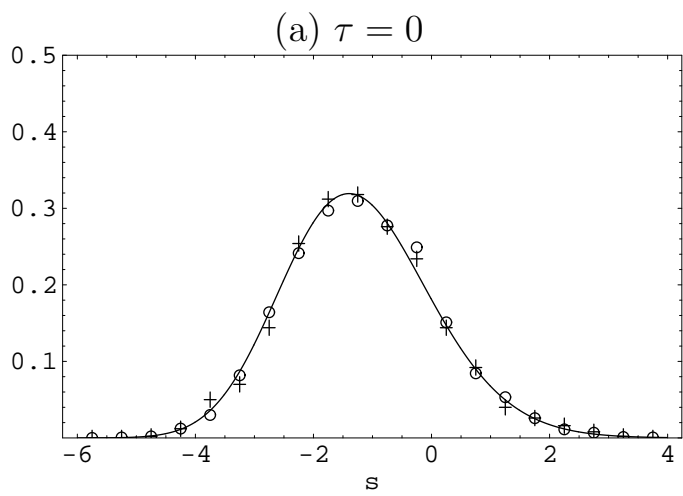


Figure 4

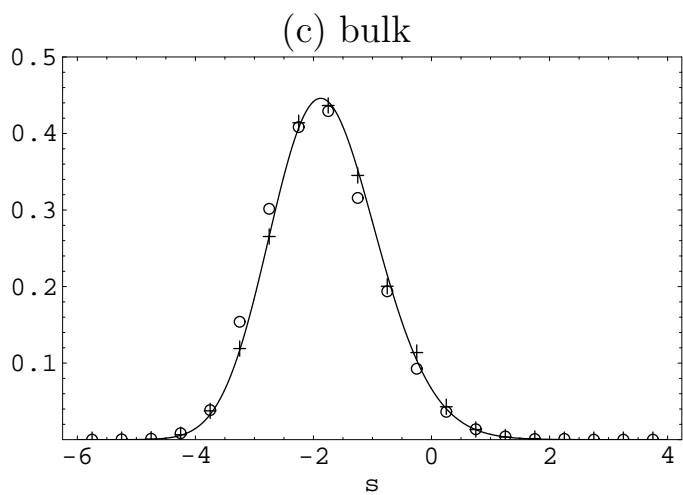
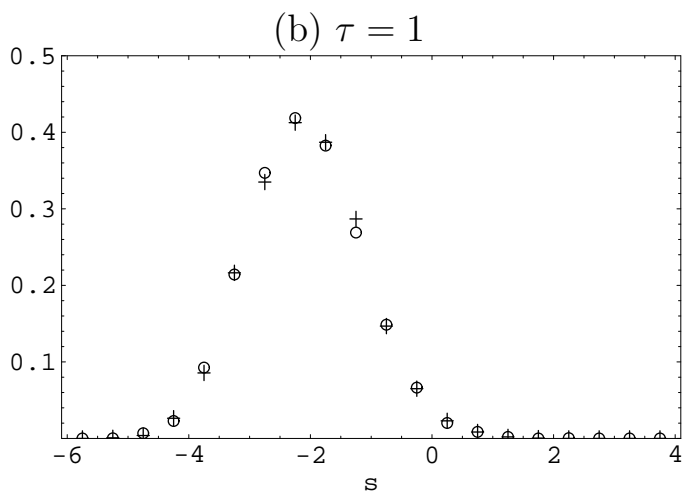
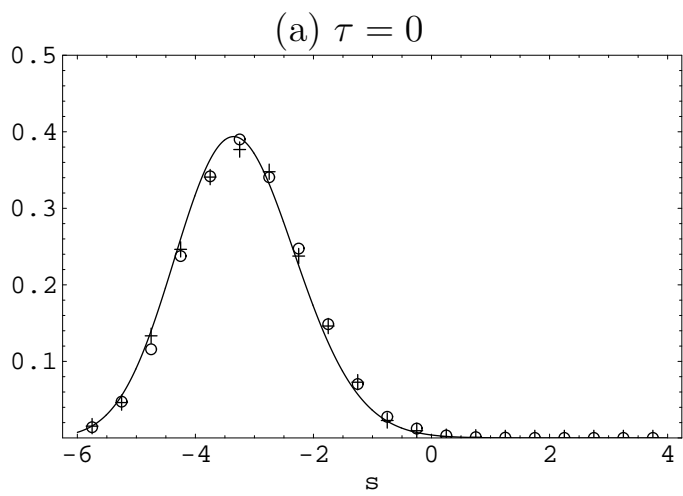


Figure 5

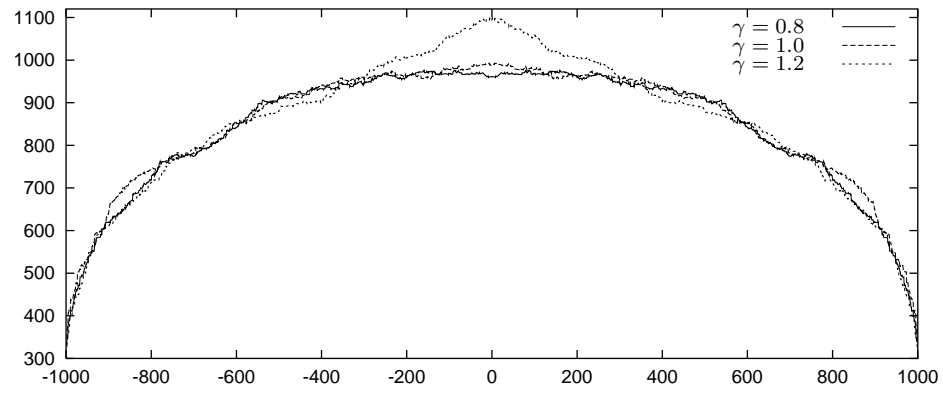


Figure 6

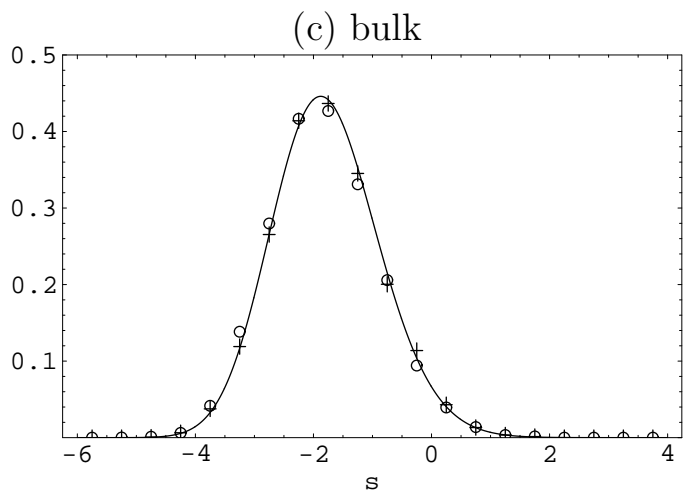
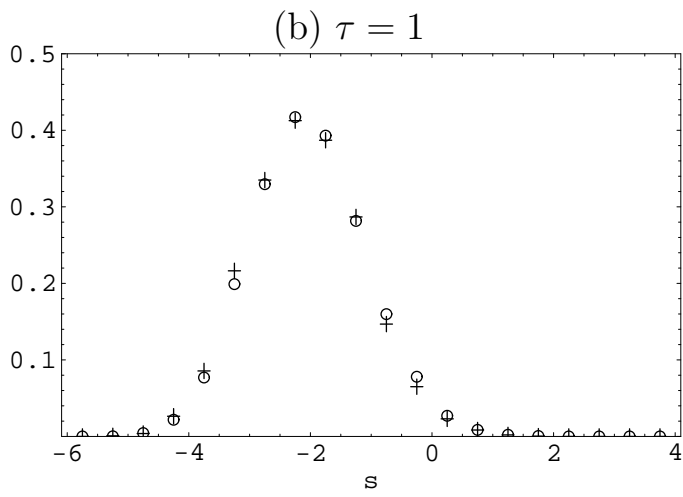
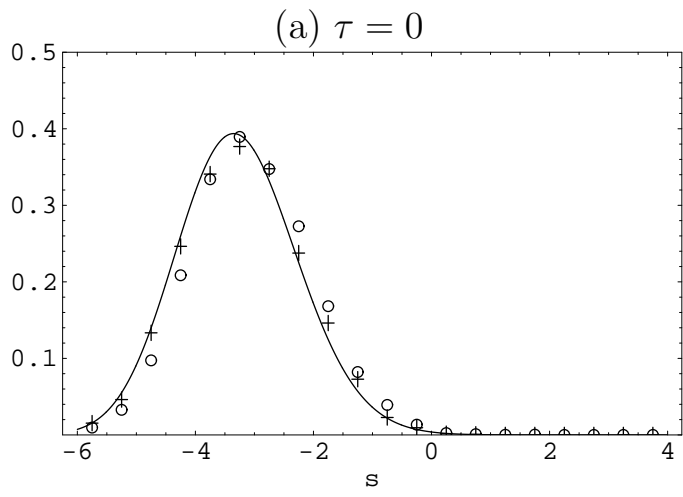


Figure 7

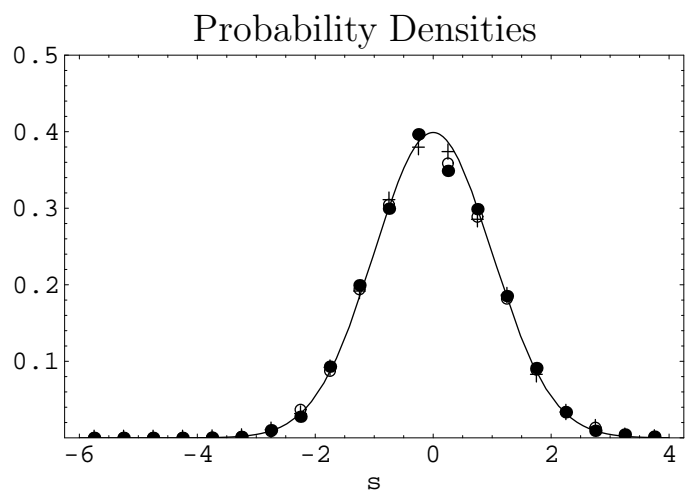


Figure 8